Model development to describe the heterogeneous kinetics of apolipoprotein B and triglyceride in hypertriglyceridemic subjects

P. Hugh R. Barrett,[1] Nome Baker,[2] and Paul J. Nestel

CSIRO, Division of Human Nutrition, Kintore Avenue, Adelaide, SA 5000, Australia

Abstract The heterogeneous nature of very low density lipoprotein (VLDL) metabolism in hypertriglyceridemia gives rise to complex kinetics when labeled VLDL are traced. Analysis of such systems benefits from the simultaneous study of several metabolically discrete subfractions which are then integrated. We have studied the kinetics of VLDL and intermediate density lipoprotein (IDL) apoprotein B and triglyceride simultaneously by injecting homologous ^{125}I-labeled VLDL1 and ^{131}I-labeled VLDL2 and [2-^{3}H]glycerol intravenously in three diverse type IV hyperlipoproteinemic subjects. An additional type IV subject received only [2-^{3}H]glycerol. Specific radioactivities were measured in: VLDL1-triglyceride and -apoB, VLDL2-triglyceride and -apoB, and in each corresponding subfraction after further separation into heparin-Sepharose-bound and -unbound fractions. ApoB and triglyceride specific radioactivities were also measured in IDL. Analysis of the kinetics of apoB in the unbound fractions in VLDL1 and VLDL2 showed the presence of two pools of particles, one of which turned over rapidly. The kinetics of apoB in the bound fractions in VLDL1 and VLDL2 were, in contrast, dominated by a large slowly turning over pool of particles that resembled the kinetics of whole VLDL. Evidence of a partial precursor-product relationship between the unbound and bound fractions suggested that the former was richer in nascent-like particles, while the latter contained more remnant particles. However, triglyceride specific radioactivity curves for both unbound and bound fractions showed initial rapid rises and broad peaks, indicating that the bound fraction also contained a substantial proportion of nascent-like particles. Using multicompartmental analysis, a model was constructed to account for the kinetics of both apoB and triglyceride in all fractions of VLDL and in IDL. The model comprises two parallel delipidation pathways that supply a common remnant pool with these features: *1*) multiple direct inputs of particles into plasma at VLDL2 and IDL levels; *2*) heterogeneous triglyceride precursor pools leading to different rates of labeling of VLDL1 and VLDL2; *3*) very substantial delipidation of VLDL2 particles; *4*) substantial early removal of VLDL2 particles prior to conversion to IDL and; *5*) triglyceride production rates somewhat higher than previously reported. The inclusion in the model of the rapidly turning over pool of triglyceride-rich particles, identified in the heparin-unbound fraction, suggests that values for triglyceride production in man have been underestimated. —**Barrett, P. H. R., N. Baker, and P. J. Nestel.** Model development to describe the heterogeneous kinetics of apolipoprotein B and triglyceride in hypertriglyceridemic subjects. *J. Lipid Res.* 1991. **32:** 743–762.

Supplementary key words triglyceride-rich particles • very low density lipoprotein • intermediate density lipoprotein

Hypertriglyceridemia is a relatively common disorder that encompasses a variety of disease states. The molecular basis for the expansion in the pool of triglyceride-rich very low density lipoproteins (VLDL) undoubtedly will be shown to be diverse. One approach has been to investigate by kinetic analysis the broader definition of hypertriglyceridemia as a state of either increased production or diminished removal; both processes have been implicated (1). Several multicompartmental models have been published recently, based on the nature of the distribution and disappearance of radiolabeled VLDL triglyceride and, or VLDL apolipoprotein (apoB). These models have provided important insights into the regulation of VLDL production and removal and represent a physiological counterpart to the knowledge generated at the cellular and molecular levels.

Despite the marked heterogeneity of hypertriglyceridemia in general and of the class of lipoproteins designated as VLDL, several publications, notably by Eaton, Allen, and Schade (2), Packard et al. (3), Fisher et al. (4), Beltz et al. (5), Zech et al. (6) and Berman et al. (7) have described models in humans that share a number of essential characteristics and also significantly extend the earlier, simpler models. The more sophisticated and complex models have been derived from the integration of several individual described subsystems. It is clear that much more information is obtained by fractionating the VLDL species into putative, metabolically discrete units in order to define their specific kinetic characteristics.

Abbreviations: HDL, high density lipoprotein; VLDL, very low density lipoprotein; IDL, intermediate density lipoprotein; TG, triglyceride; FCR, fractional catabolic rate.

[1]To whom correspondence should be addressed at: Center for Bioengineering, FL-20, University of Washington, Seattle, WA 98195.

[2]Present address: John Muir Cancer and Aging Institute, 2055 North Broadway, Walnut Creek, CA 94596.

We have utilized this approach by combining two techniques for the physiochemical separation of VLDL, ultracentrifugation and affinity chromatography. We have previously shown that VLDL can be separated by heparin-Sepharose chromatography into particles that show partial precursor-product characteristics (8). We have simultaneously labeled VLDL triglyceride endogenously with [2-^{3}H]glycerol and labeled VLDL apoB (the key structural protein) exogenously with two further radioisotopes for the larger and smaller VLDL particles. This has provided metabolic data on the triglyceride and apoB moieties of four separate VLDL species. The integration into a single model of information so obtained in four patients has confirmed several aspects present in other multicompartmental models and has also highlighted some new observations.

METHODS

Four hypertriglyceridemic (type IV phenotype) subjects gave informed consent for the study. Their ages, body weights, heights, and plasma lipid profiles are presented in **Table 1**. None of the subjects was being treated with drugs and in all, the hypertriglyceridemia was primary. Only hypertriglyceridemic subjects were used in this study to provide enough lipoprotein material to allow the measurement of multiple classes of VLDL.

Each subject, with the exception of J who received only [2-^{3}H]glycerol, received an intravenous injection of autologous ^{125}I-labeled VLDL (VLDL1, S_f 60–400), ^{131}I-labeled VLDL (VLDL2, S_f 20–60), and [2-^{3}H]glycerol in order to study the kinetics of apoB and of triglyceride in those lipoprotein fractions.

Prior to obtaining VLDL for iodination, the subjects were placed for 4 days on a constant alcohol-free diet aimed to reduce dietary fat particles (30% energy as fat, 50% energy as carbohydrate, 20% energy as protein). The carbohydrate content of this diet is that of the average Australian diet. Lipoproteins for radioiodination were isolated from 30 ml plasma obtained after the subjects had fasted overnight. Chylomicrons ($S_f > 400$) were removed by ultracentrifugation of plasma at 20,000 *g* for 30 min. VLDL1 and VLDL2 were isolated in a Beckman 50Ti anglehead rotor by ultracentrifugation for 2 h and 16 h, respectively, at 105,000 *g*, 15°C, and d < 1.006 g/ml (0.15 M NaCl, 0.01% Na_2 EDTA, and gentamycin, 80 mg/l). Lipoprotein fractions were iodinated with ^{125}I or ^{131}I using the ICl technique of McFarlane (9) as modified by Fidge and Poulis (10). Lipoprotein-bound iodine was separated from free iodine initially by gel filtration on a column of Sephadex G-50, with 0.15 M NaCl and 1.0 mM EDTA as the eluting solution. This was followed by dialysis against numerous changes of buffered saline over a period of 4 h.

TABLE 1. Clinical data of subjects

Subject	Clinical State	Age	Sex	Weight	Height	Plasma Cholesterol	Plasma Triglyceride
		yr		*kg*	*cm*	*mg/dl*	
F	Type IV	54	M	98	174	264 ± 17	347 ± 39
K	Type IV	66	M	79	172	299 ± 22	870 ± 93
H	Type IV	61	M	71	160	230 ± 13	277 ± 35
J	Type IV	64	M	79	178	255 ± 16	436 ± 14

Mean ± SD.

Radioiodinated autologous lipoproteins for reinjection were passed through a 0.45-μm Millipore filter after iodination. An aliquot of the lipoprotein was routinely selected for measurement of radioactivity and tested for the presence of pyrogens using the Limulus kit (Mallinckrodt, St. Louis).

During the 48-h period of the study, the subjects who were ambulant ate very little fat (<5% energy) and a total of 85% of their required energy was derived from carbohydrate (68%) and protein (17%). This diet had been modified from that designed by Grundy et al. (11) to minimize alimentary particles and VLDL overproduction. During the course of each turnover study, plasma VLDL triglyceride and apoB concentrations remained constant. Subjects received labeled lipoproteins, 50–100 μCi ^{125}I-labeled VLDL1, 30–60 μCi ^{131}I-labeled VLDL2, and 300 μCi [2-^{3}H]glycerol, injected via an indwelling catheter placed in a forearm vein. All radioactive materials were injected as a bolus. Up to 12 blood samples were collected within the first 6 h, thereafter less frequently for up to 48 h. Subject F, however, was studied for only 14 h due to the administration of medication that would have perturbed "normal" lipid metabolism. Potassium iodide was given daily to prevent thyroidal uptake of radioiodine.

Blood samples were collected into 0.01% Na_2 EDTA tubes and plasma was isolated by centrifugation at 1000 *g* at 4°C for 15 min. Gentamycin sulfate (0.10 mg/ml) and 0.01% Na_2 EDTA were added to plasma samples which were kept at 4°C until further processed. VLDL1 and VLDL2 were isolated as described above. IDL was isolated by adjusting the VLDL2 infranate to a density of 1.019 g/ml and centrifuging for 18 h. In addition, LDL was isolated after adjusting the IDL infranate to a density of 1.063 g/ml and centrifuging for 24 h. Isolated IDL and LDL were dialyzed against 0.15 M NaCl.

Aliquots of both VLDL1 and VLDL2 were subfractionated by heparin-Sepharose affinity chromatography (12) into two populations of particles; a heparin-Sepharose-bound (the "bound" fraction) and heparin-Sepharose unbound (the "unbound" fraction) fraction. Earlier studies (8, 13) have demonstrated that the apoE/apoC ratio of the bound fraction is significantly greater than that of

the unbound fraction. Heparin Sepharose CL-6B affinity columns (1.0 × 30.0 cm) were equilibrated with 0.05 M NaCl, 2 mM PO_4^{3-}, pH 7.4. Samples containing between 2 and 3 mg of protein were dialyzed against the starting buffer. The unbound VLDL was eluted, with the starting buffer, at a flow rate of 20 ml/h at 4°C, and collected in 2-ml fractions. After approximately 2 h when the absorbance of the fractions, measured at 280 nm, was zero, a 0.8 M NaCl, 2 mM PO_4^{3-} buffer was used to elute the bound VLDL. All fractions were measured at 280 nm and pooled into two groups. Measures of total protein showed recoveries generally greater than 85%.

Plasma and lipoprotein fractions were assayed for triglyceride and cholesterol concentrations in a Technicon Auto-Analyser (AA-II) (14). Immunoassays for the determination of apoB concentration were carried out by the rocket immunoelectrophoretic procedure described by Reardon et al. (15). Each of the above analyses was done in duplicate using replicate serial plasma samples from each subject to determine mean values.

ApoB and triglyceride specific radioactivity measurements were made on all lipoprotein fractions and subfractions, without concentrating the pooled eluates. ApoB was precipitated from lipoprotein samples using a modification of the method of Egusa et al. (16). Between 500 and 700 μg of protein, in about 1 ml, was mixed with an equal volume of 100% isopropanol. After vigorous mixing, samples were incubated at room temperature overnight and centrifuged at 1000 *g* for 30 min. The supernatant was aspirated and the pellet was washed with a volume of 100% isopropanol. The sample was recentrifuged and the supernatant was discarded. After delipidation the samples were centrifuged, and the pellets were dried and dissolved in 1 N NaOH. Radioactivity of the apoB was measured in a gamma scintillation counter which was standardized for simultaneous determination of ^{125}I and ^{131}I.

To determine triglyceride specific radioactivities, neutral lipids were extracted from samples (17) and triglyceride concentrations were determined using the method of Neri and Frings (18). Aliquots of the isopropanol extract produced by this method were dried, redissolved in scintillation fluid, and assayed for radioactivity.

Kinetic analysis

Kinetic analyses of both the apoB and triglyceride specific radioactivity curves and calculation of transport rates based upon observed pool sizes and steady state assumptions were carried out using the SAAM and CONSAM programs (19, 20). After the initial parameter estimations, the parameters of the model were allowed to adjust to obtain a least-squares fit to the data. The development of the model is described in the Results section and a complete summary of the parameters derived by multicompartmental analysis of the data using the model shown in Fig. 9 is given in the Appendix, for each of the four subjects.

RESULTS

Lipoprotein composition

Table 2 describes for the four subjects the plasma triglyceride, cholesterol, and apoB concentrations in VLDL1 (S_f 60-400), VLDL2 (S_f 20-60), IDL, and LDL. Triglyceride, apoB, and cholesterol concentrations in both VLDL fractions displayed the marked heterogeneity that is known to exist in the heterogeneous disorder, type IV hyperlipoproteinemia. The larger VLDL1 particles contained the same or, in subjects K and J, a greater amount of triglyceride, per apoB, than the smaller VLDL2 particles. Examination of the data in this table reveals that in three of the four subjects most of the apoB mass, and thus the majority of particles, in the VLDL fraction were within the VLDL2 range, the exception being the most hyperlipidemic subject, subject K. The cholesterol/triglyceride ratios indicate, as expected (8), that this ratio was higher in the VLDL2 than in the VLDL1 fraction. The LDL data were consistent with findings in hypertriglyceridemic subjects, showing normal cholesterol and apoB concentrations and relative triglyceride enrichment (21).

Heparin-Sepharose affinity chromatography

Each VLDL fraction was separated by heparin-Sepharose affinity chromatography into two populations of particles that were either unretained (unbound) or re-

TABLE 2. Lipid and apolipoprotein B concentrations of lipoprotein fractions

Subject	Lipoprotein Fraction	Triglyceride	ApoB	Cholesterol	TG/ApoB	Chol/TG
		mg/dl				
F	VLDL1[a]	82 ± 17	6.8 ± 1.2	12 ± 1.7	12.0	0.15
	VLDL2[a]	168 ± 33	14 ± 2.4	40 ± 4.2	12.3	0.24
	IDL	14 ± 4	7.0 ± 0.9	16 ± 1.4	2.1	1.10
	LDL	17 ± 2	85 ± 9.9	114 ± 11	0.2	6.54
K	VLDL1	507 ± 67	35 ± 5.2	136 ± 14	14.6	0.27
	VLDL2	212 ± 14	20 ± 1.9	72 ± 5.1	10.5	0.34
	IDL	33 ± 5	11 ± 1.6	22 ± 3.2	2.9	0.66
	LDL	28 ± 5	44 ± 5.8	52 ± 7.4	0.6	1.87
H	VLDL1	46 ± 10	7.6 ± 1.4	9.1 ± 1.2	6.0	0.19
	VLDL2	160 ± 25	28 ± 6.5	41 ± 5.4	5.7	0.25
	IDL	24 ± 5	11 ± 1.5	18 ± 2.1	2.1	0.76
	LDL	28 ± 2	91 ± 5.8	87 ± 5.8	0.3	3.12
J	VLDL1	105 ± 10	4.5 ± 1.2	15 ± 0.9	23.4	0.14
	VLDL2	249 ± 14	22 ± 3.3	47 ± 2.7	11.6	0.19
	IDL	17 ± 3	6.7 ± 0.9	11 ± 0.2	2.6	0.66
	LDL	17 ± 2	36 ± 5.1	73 ± 1.6	0.5	4.35

Values given as mean ± SD.
[a]VLDL1, S_f 60-400; VLDL2, S_f 20-60.

TABLE 3. Triglyceride and apolipoprotein B concentrations of heparin-Sepharose fractionated VLDL

Subject	VLDL Fract.	Unbound Fraction			Bound Fraction		
		Triglyceride	ApoB	TG/ApoB	Triglyceride	ApoB	TG/ApoB
		mg/dl			*mg/dl*		
F	VLDL1[a]	31 ± 13	2.0 ± 0.1	15.3[b]	51 ± 25	4.8 ± 1.3	10.6[b]
	VLDL2[a]	56 ± 27	1.3 ± 0.8	43.1	112 ± 43	12 ± 3.1	9.0
K	VLDL1	381 ± 61	20 ± 5.8	18.9	126 ± 29	14 ± 3.3	8.8
	VLDL2	106 ± 12	7.6 ± 1.4	13.9	106 ± 15	13 ± 1.7	8.5
H	VLDL1	7.4 ± 2.7	0.65 ± 0.2	11.4	38 ± 4.5	7.0 ± 1.8	5.5
	VLDL2	80 ± 11	11 ± 3.2	7.4	80 ± 8.9	17 ± 3.3	4.7
J	VLDL1	68 ± 18	1.7 ± 0.2	39.7	38 ± 6.3	2.8 ± 0.9	13.5
	VLDL2	145 ± 18	7.6 ± 1.7	19.1	104 ± 15	14 ± 1.9	7.5

Values given as mean ± SD.
[a]VLDL1, S_f 60-400; VLDL2, S_f 20-60.
[b]The triglyceride/apoB ratios of the unfractionated VLDL fractions shown in Table 2 are the weighted average of the unbound and bound triglyceride/apoB ratios presented in this Table.

tained (bound). The data in **Table 3** describe the distribution of triglyceride and apoB in the four subfractions. As noted in the footnote to Table 3, the TG/apoB ratios presented in Table 2 represent the weighted mean of those presented in Table 3. On the basis of the apoB concentrations there appeared to be more particles in the bound than in the unbound fractions with one exception (subject K, VLDL1). In both VLDL1 and VLDL2 the unbound fractions had higher TG/apoB ratios than found in the bound fractions. This is consistent with the conclusion of Nestel et al. (8) that the bound fraction contains products of the unbound fraction. In all subjects, except for subject F, the TG/apoB ratios of unbound and bound fractions in the VLDL1 fraction were greater than for the corresponding fractions in the VLDL2 fractions. However, the TG/apoB ratio of the bound VLDL1 was less than that for the unbound VLDL2 fraction, suggesting that the latter was not exclusively a product of VLDL1. A comparison of the proportions of unbound:bound apoB shows that, except for subject H and perhaps subject J, the ratios were greater in the VLDL1 fraction than in the VLDL2. Both fractions (VLDL1 and VLDL2), therefore, contained a population of both unbound and bound particles, and, in subjects F and K (and J), as the particles became smaller the proportion of bound particles increased.

Lipoprotein kinetics

To study the metabolism of VLDL through to IDL, autologous ^{125}I-labeled VLDL1 and ^{131}I-labeled VLDL2 were injected together with a bolus of [2-^{3}H]glycerol. Subject J, however, received only [2-^{3}H]glycerol. The apoB and triglyceride moieties were isolated and specific radioactivity curves were produced for both apoB and TG in VLDL1, VLDL2, and IDL. (Due to the relatively short period of the study LDL data are not included.) Subjects F and K are used here to illustrate the two general types of data observed in the four subjects studied and to illustrate the goodness of fit of the model in Fig. 9 using the SAAM analysis.

Apolipoprotein B kinetics in VLDL1, VLDL2, and IDL

Specific radioactivity curves of unfractionated plasma VLDL1 and VLDL2 apoB were generally monoexponential (**Fig 1, Fig. 2, and Fig. 3**), with the exception of subject H where a biexponential curve was observed. The unfractionated VLDL1 and VLDL2 specific radioactivity curves, which were measured independently, represent the weighted mean specific radioactivity function of the unbound and bound apoB fractions. This is illustrated in Figs. 1-3 for VLDL1 and VLDL2.

Examination of the plasma disappearance curves for the unbound and bound VLDL fractions (Figs. 1-3) were, however, more revealing than those of unfractionated VLDL, for which two patterns were observed. In subject F the unbound plasma VLDL1 and VLDL2 apoB disappearance curves were biexponential in shape and revealed the presence of a rapidly turning over component within these fractions. The terminal slope of the unbound curves was the same as that of the bound fractions. Similar biexponential curves, the minor slow components of which parallel the bound fraction, were also seen in the unbound VLDL1 of subject H. However the unbound plasma VLDL2 apoB disappearance curves were monoexponential in subjects H and K and in VLDL1 of subject K (Fig. 1), and the slope of the unbound fraction was greater than that of the bound fraction, which exhibited a delay prior to its fall (Figs. 1-3).

The initial specific radioactivity of the unbound fraction was lower than that of the bound in subjects F (Figs.

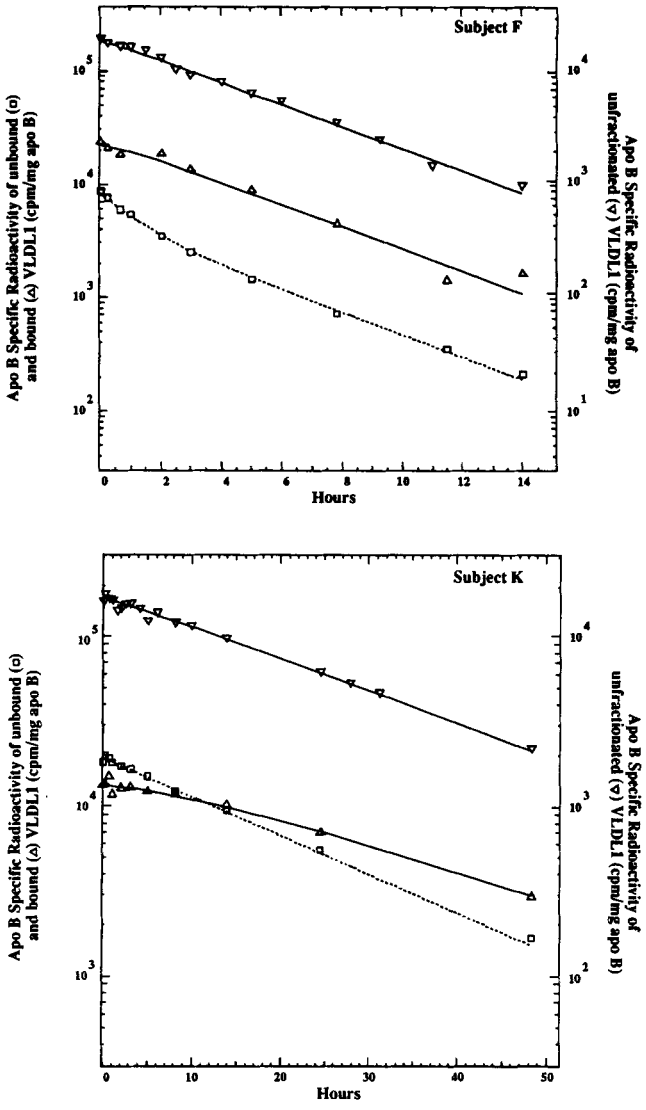

Fig. 1. Specific radioactivity of ^{125}I-labeled apoB unfractionated (▽), heparin-Sepharose unbound (□), and heparin-Sepharose bound plasma VLDL1 (△) for subjects F and K after i.v. injection of unfractionated autologous ^{125}I-labeled VLDL1. The symbols represent observations while the curves show the fits to the model (Fig. 9) using SAAM. Left ordinate, fractionated VLDL1; right ordinate, unfractionated VLDL1.

1 and 3) and H which would obscure the expected precursor-product relationship between the unbound and bound fractions in these subjects. Although labeled together, the unbound and bound apoB specific radioactivities, which should theoretically be equal, were often different, a feature seen in the earlier study of Nestel et al. (8) as well. The difference between the initial specific radioactivities of the unbound and bound fractions could be due to changes in the mass distribution of the various particle populations within the subject during the period when VLDL was isolated, iodinated, and reinjected. Alternatively, these differences may be due to the nonuniform labeling of apoB, a notion that has been considered for many years and for which there is now some evidence (22).

Table 4 shows the fast and slow components of the VLDL unbound apoB specific radioactivity curves in subjects F and H (VLDL1 only). These plasma disappearance curves have been peeled to reveal the rapidly turning over components that were observed only in these subjects. The unbound VLDL fractions of some of the subjects described in the studies of Nestel et al. (8) showed similar kinetic behavior. The slope of the faster component in these subjects is of the order of 1 per hour. The slower terminal slope (between 0.1 and 0.2 per hour) of the unbound apoB curve was similar to the monoexponential slope of the bound fraction.

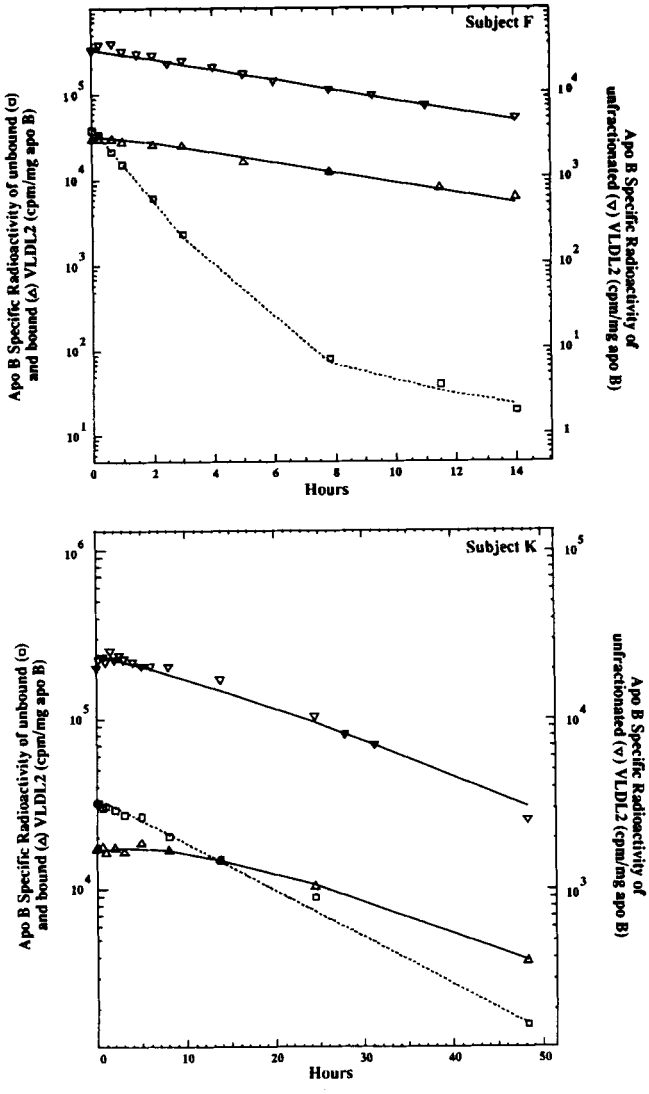

Fig. 2. Specific radioactivity of ^{125}I-labeled apoB unfractionated (▽), heparin-Sepharose unbound (□), and heparin-Sepharose bound plasma VLDL2 (△) for subjects F and K after i.v. injection of unfractionated autologous ^{125}I-labeled VLDL1. The symbols represent observations while the curves show the fits to the model (Fig. 9) using SAAM. Left ordinate, fractionated VLDL2; right ordinate, unfractionated VLDL2.

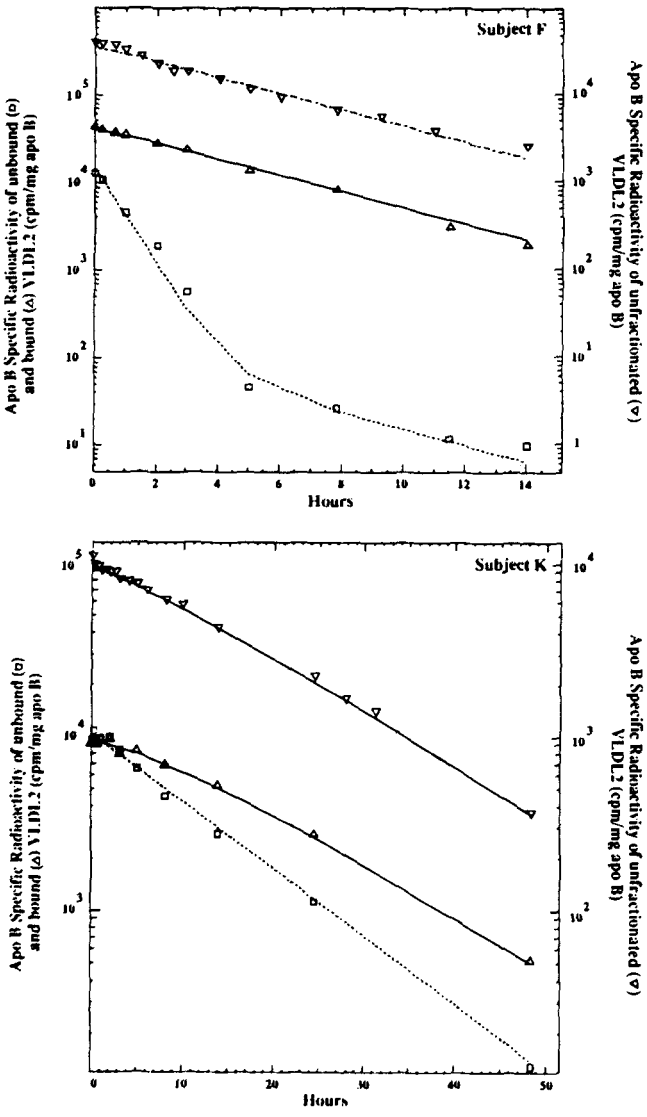

Fig. 3. Specific radioactivity of ^{131}I-labeled apoB unfractionated (▽), heparin-Sepharose unbound (□), and heparin-Sepharose bound plasma VLDL2 (△) for subjects F and K after i.v. injection of unfractionated autologus ^{125}I-labeled VLDL1. The symbols represent observations while the curves show the fits to the model (Fig. 9) using SAAM. Left ordinate, fractionated VLDL2; right ordinate, unfractionated VLDL2.

The apoB kinetics of the IDL fraction revealed the transfer of mass from the VLDL fractions to those of a higher density. In each subject the specific radioactivity curve exhibited an initial rise, followed by a peak and a slowly decaying tail (**Fig. 4** and **Fig. 5**). Of interest is the observation that the ^{131}I-labeled IDL fraction (Fig. 5) reached its peak radioactivity earlier than that of the ^{125}I-labeled IDL (Fig. 4), indicating that less time was involved in the conversion of VLDL2 to IDL compared to VLDL1. In addition, observation that the peak specific radioactivity of the ^{125}I-labeled IDL fraction did not cross the specific radioactivity curve of the VLDL2 fraction suggested direct secretion of particles into the IDL fraction. In contrast, this relationship for the same fractions labeled with ^{131}I suggested little or no direct secretion into the IDL fraction. That the relationships between the VLDL2 and IDL specific radioactivity curves were different for the two tracers could be accounted for by metabolic channeling (3) and the heterogeneous nature of the VLDL2, and presumably other fractions. In brief, if a smaller fraction of the ^{125}I-labeled VLDL2, originally derived from VLDL1, is converted to IDL than those particles originating in the VLDL2, namely the ^{131}I-labeled VLDL2, then this would account for the different relationships we have observed.

Triglyceride kinetics in VLDL1, VLDL2, and IDL

Very low density lipoprotein triglyceride kinetics were studied after the administration of a bolus of [2-^{3}H]glycerol, which is endogenously incorporated into the triglyceride moiety of lipoproteins. The triglyceride specific radioactivity curves of unbound and bound fractions, both in VLDL1 (**Fig. 6**) and in VLDL2 (**Fig. 7**) exhibited a number of similar features. All triglyceride curves displayed an initial rapid rise in specific radioactivity, a peak, and a subsequent fall in radioactivity as has been commonly reported by others (6). The triglyceride specific radioactivity curves of unfractionated VLDL1 and VLDL2 showed similar features. Each represents the summation (weighted mean specific radioactivity) of the corresponding unbound and bound curves.

In the VLDL1 of subject H and both VLDL fractions of subject J, a slowly disappearing tail was seen at later times. This tail, which has often been observed in VLDL triglyceride curves and which is thought to represent the kinetics of a slowly turning over liver triglyceride precursor, was observed neither in VLDL1 (Fig. 6) nor in VLDL2 (Fig. 7) of subjects F and K, nor in VLDL2 of subject H. The duration of the study was too short for this feature to have been detected in subject F.

TABLE 4. Rate constants of curve-peeled components of the VLDL unbound apoB fractions of subjects F and H

		Fast		Slow	
		h^{-1}	%[a]	h^{-1}	%
F	VLDL1	0.77 (0.12)	57.3	0.21 (0.01)	42.7
F	VLDL2	1.21 (0.04)	99.7	0.09 (0.03)	0.3
H	VLDL1	1.75 (0.13)	94.9	0.10[b]	5.1

Values in parentheses are ± SD.
[a]Percentage of fast and slow components based upon relative intercepts with the ordinate.
[b]Assigned value used to fit tail of decay curve.

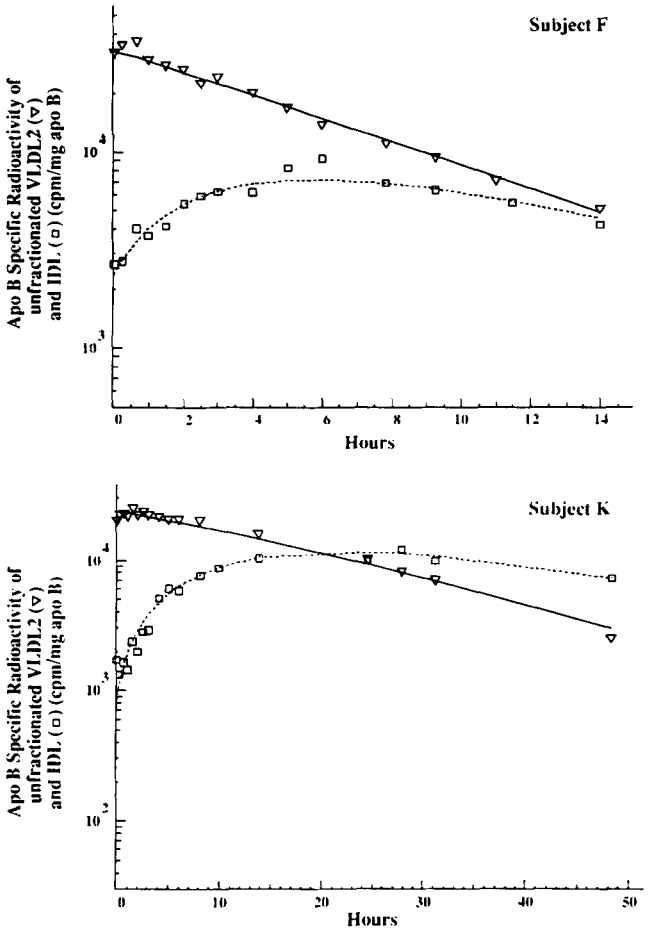

Fig. 4. Specific radioactivity of ^{125}I-labeled apoB unfractionated VLDL2 (▽) and IDL (□) for subjects F and K after i.v. injection of unfractionated ^{125}I-labeled VLDL1. The symbols represent observations while the curves show the fits to the model (Fig. 9). The fits to the data were derived by coupling the ^{125}I-labeled apoB and triglyceride VLDL2 and IDL data.

The rising portions of both the VLDL1 and VLDL2 triglyceride specific radioactivity curves, all six of which (unfractionated, bound, and unbound) had similar initial rates in each individual were not preceded by any significant delay. This indicates that the intrahepatic processes of glycerol incorporation into triglyceride, packaging of triglyceride into VLDL particles, and secretion of nascent VLDL particles by way of the Golgi apparatus were unexpectedly rapid. Despite their similar characteristics, the maximum specific radioactivity of the VLDL2 fraction was higher (21–85%) than that of the VLDL1 fraction and was reached 0.5–1.0 h later. The higher maximum for VLDL2 triglyceride specific radioactivity suggests that there was probably at least as much direct input of triglyceride into the VLDL2 fraction as there was into the VLDL1 fraction.

The specific radioactivity curve of the bound fraction peaked at about the same time as that of the unbound fraction (Figs. 6 and 7). In general, after reaching its peak, the specific radioactivity of the unbound fraction fell quite rapidly resulting in the curve falling below that of the bound fraction. The fall in triglyceride specific radioactivity of the bound fraction was slower than that of the unbound. The unbound and bound fractions displayed steeply rising initial slopes suggesting that each fraction contained a directly secreted, nascent-like component.

In addition to the triglyceride kinetics of the VLDL fraction, the kinetics of IDL triglyceride were studied. Intermediate density lipoprotein triglyceride kinetics generally exhibited the same features as the VLDL-triglyceride kinetics. There were, however, some differences, the rise of the specific radioactivity curve being slower (**Fig. 8**) than that of the VLDL2. Although the time to peak specific radioactivity was longer than that observed for the VLDL fractions, the tail of the IDL

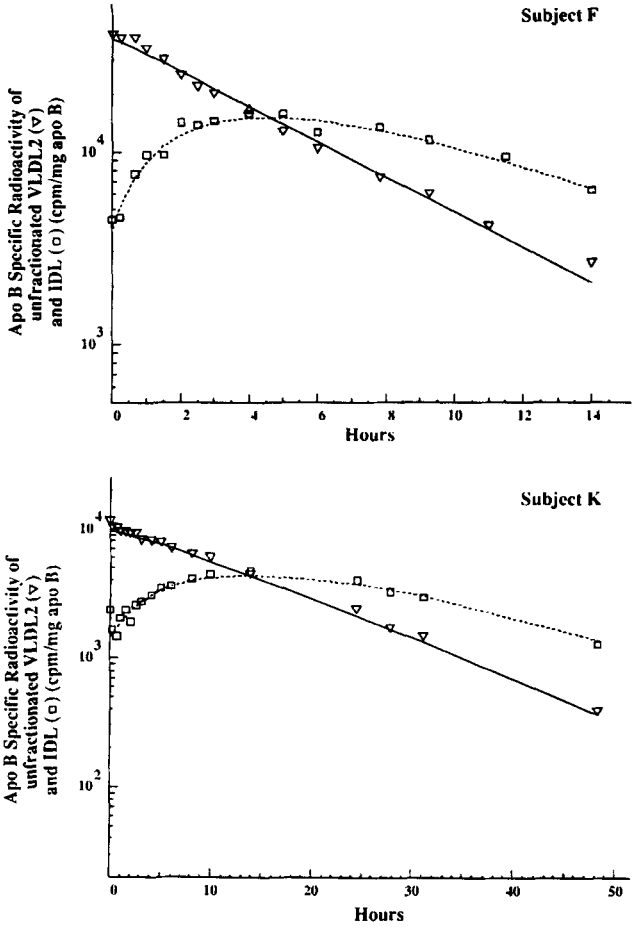

Fig. 5. Specific radioactivity of ^{131}I-labeled apoB unfractionated VLDL2 (▽) and IDL (□) for subjects F and K after i.v. injection of unfractionated ^{131}I-labeled VLDL2. The symbols represent observations while the curves show the fits to the model (Fig. 9). The fits to the data were derived by coupling the ^{131}I-labeled apoB and triglyceride VLDL2 and IDL data.

curve appeared to be slower than that of the VLDL fraction; however, its shape was consistent with the hypothesis that most IDL triglyceride is derived from VLDL2 triglyceride and that either the precursor VLDL2 triglyceride compartment is rate-limiting or that IDL triglyceride turns over more slowly than the VLDL2 triglyceride precursor.

Kinetic analysis and model development

Initially we assumed, based upon the work of Nestel et al. (8), that heparin-Sepharose affinity chromatography separates VLDL particles into nascent-rich (unbound) and remnant-rich (bound) fractions, as indicated in the model. However, we recognized that "nascent-like" particles rich in TG and apoC relative to apoB and cholesterol, properties possessed by the unbound particles (8, 13), may well differ from the lipoproteins secreted by the liver as truly nascent particles.

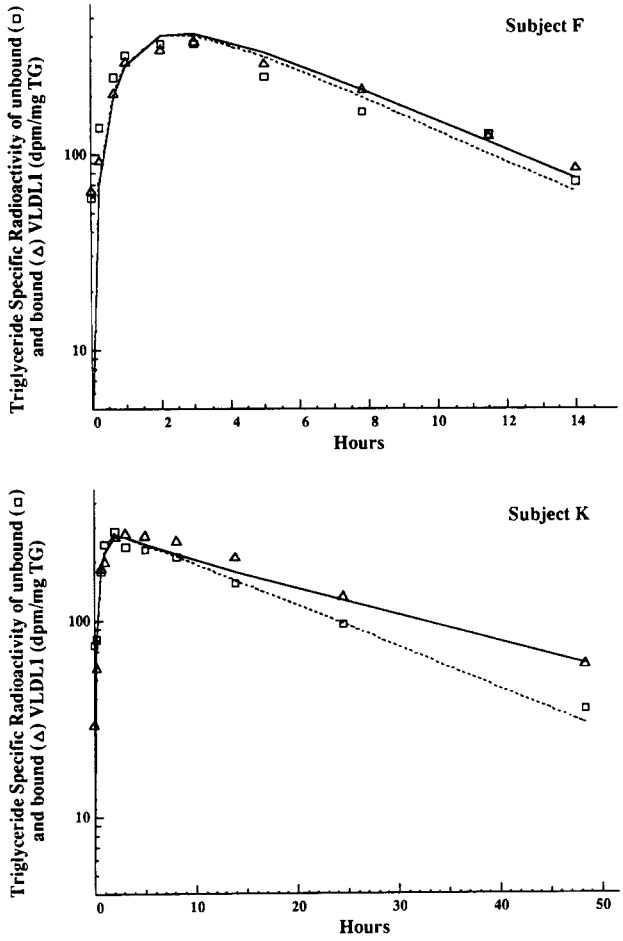

Fig. 6. Specific radioactivity curves of [^{3}H]triglyceride in heparin-Sepharose unbound (□) and bound (△) VLDL1 for subjects F and K after i.v. injection of [2-^{3}H]glycerol. The symbols represent observations while the curves show the fits to the model (Fig. 9). The fits to the data were derived by coupling the ^{125}I-labeled apoB and triglyceride VLDL1 data.

By labeling VLDL1 apoB with ^{125}I and VLDL2 apoB with ^{131}I and by observing the kinetic behavior of labeled triglycerides in each subfraction after injecting [2-^{3}H]glycerol, we expected to be able to follow the transport of the apoB and TG moieties from VLDL1 down the delipidation chain to LDL particles, as well as to ascertain the extent of direct input of both apoB and TG into the system at each stage of the process. We also hoped to evaluate the relative contributions of nascent VLDL1, remnant VLDL1, and nascent VLDL2 to the formation of VLDL2 remnants.

Basic to the experimental design were the assumptions that the liver triglyceride compartment serving as the precursor of the nascent particles was rate-limiting, that this rate determined, to a large extent, the early falling slope of the plasma triglyceride specific radioactivity curve, and that the rising part of the latter was dominated by the kinetic behavior of the more rapidly turning over nascent VLDL particles.[3]

Our working model had to be modified after initial examination of the triglyceride specific radioactivity curves in the unbound and bound fractions, which clearly were inconsistent with a precursor and product relationship expected for triglycerides in the nascent and remnant compartments, respectively. Yet, based on apoB kinetic data, as noted earlier by Nestel et al. (8) and confirmed here, the apoB in the bound fraction frequently possessed the characteristics expected (23) for the product of a precursor nascent apoB compartment in the unbound fraction.

The model shown in **Fig. 9** resolved the apparent discrepancy between the kinetic behaviors of the unbound and bound VLDL triglyceride and apoB tracer data. This model deals only with the VLDL2 and IDL fractions, upon which the present analysis focuses. This model does not describe the conversion of VLDL1 to VLDL2 because of the rapid transfer of ^{125}I radioactivity into the VLDL2 fraction, which occurred almost immediately after reinjection. Although discussed more fully below, a consequence of this transfer was that VLDL1 to VLDL2 transport rates for apoB and triglyceride could not be determined. In addition, due to the relatively short duration of each study, we were not able to quantify either the turnover rate of the LDL particles or the fraction of IDL that is converted to LDL. Only if labeled LDL had been reinjected and the studies were undertaken for a longer period (10–14 days) could we have reliably estimated these parameters.

[3]The evidence in the literature that led to our making these assumptions, which differ from those made in earlier models of human plasma VLDL triglyceride synthesis and turnover, have been summarized in an article to be published elsewhere (Baker, N., H. Barrett, and P. J. Nestel, unpublished results; based on material presented at the VIIth International Conference on Atherosclerosis in 1985 and at the Annual Kinetic Workshop on Lipoprotein Kinetics and Modeling in Bethesda, 1988).

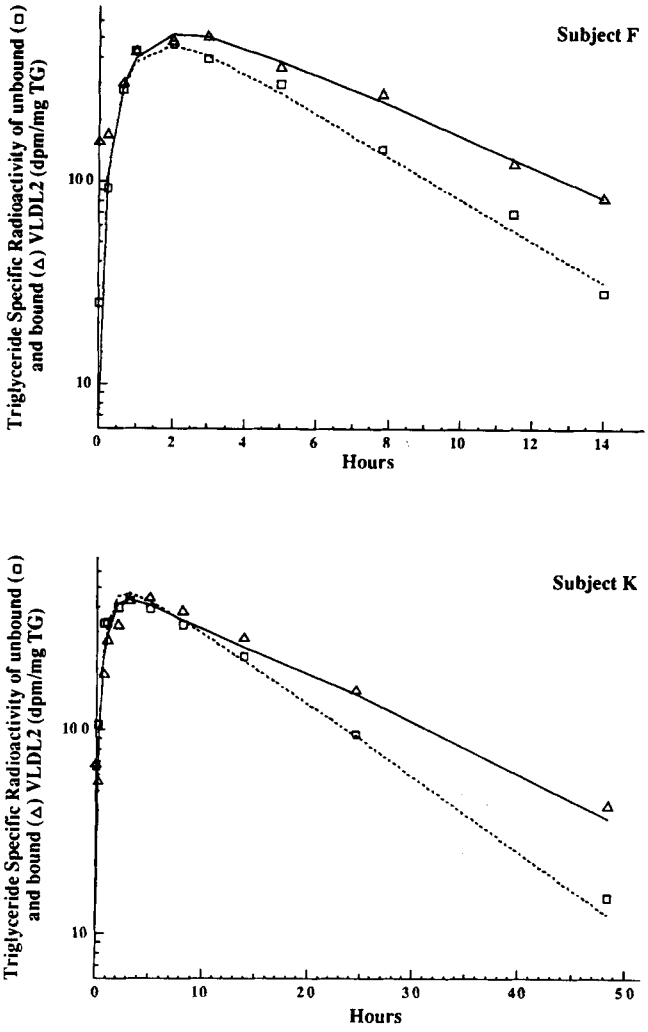

Fig. 7. Specific radioactivity curves of [^{3}H]triglyceride in heparin-Sepharose unbound (□) and bound (△) VLDL2 for subjects F and K after i.v. injection of [2-^{3}H]glycerol. The symbols represent observations while the curves show the fits to the model (Fig. 9). The fits to the data were derived by coupling the ^{131}I-labeled apoB and triglyceride VLDL2 data.

The model in Fig. 9 consists of four subsystems: glycerol, glycerol-to-triglyceride conversion, VLDL2, and IDL. The parameters of the glycerol subsystem were the same as those used by Zech et al. (6). The glycerol-to-triglyceride conversion subsystem consisted of two compartments, one with a high turnover rate (0.15–0.23 per h). This compartment accounted for most, and in some subjects all, of the radioactivity in VLDL and IDL. The more slowly turning over compartment contributes mainly to the tail of the VLDL curve which was only observed in subjects H (VLDL1 only) and J.

The VLDL2 section of the model (Fig. 9) accommodates marked differences among the subjects in the kinetic behavior of labeled apoB in the VLDL2 unbound fractions, which was also observed in the unbound VLDL1 fractions of some subjects. These differences were displayed by the presence or absence of a dominant rapid component having the approximate rate constant predicted from labeled TG data for the nascent-like particles. Similar variations among subjects can also be seen in the data presented earlier by Nestel et al. (8). Thus, in some subjects, nascent-like particles in the unbound fraction were assumed to flow to unbound remnant-like particles and then to bound remnant-like particles (C5 to C8 to C9, and C11 to C14 to C15). In these subjects the kinetics of the nascent-like particles would be masked by those of the more slowly turning over remnant-like particles. This masking occurs because exogenous labeling was used to trace VLDL particles, hence the initial specific radioactivities of the particles within the unbound fraction would be equal. When this occurs, the kinetics of the more slowly turning over particles dominate the specific radioactivity curve (23). In other subjects, the flow of unbound nascent particles was assumed to be directly to bound

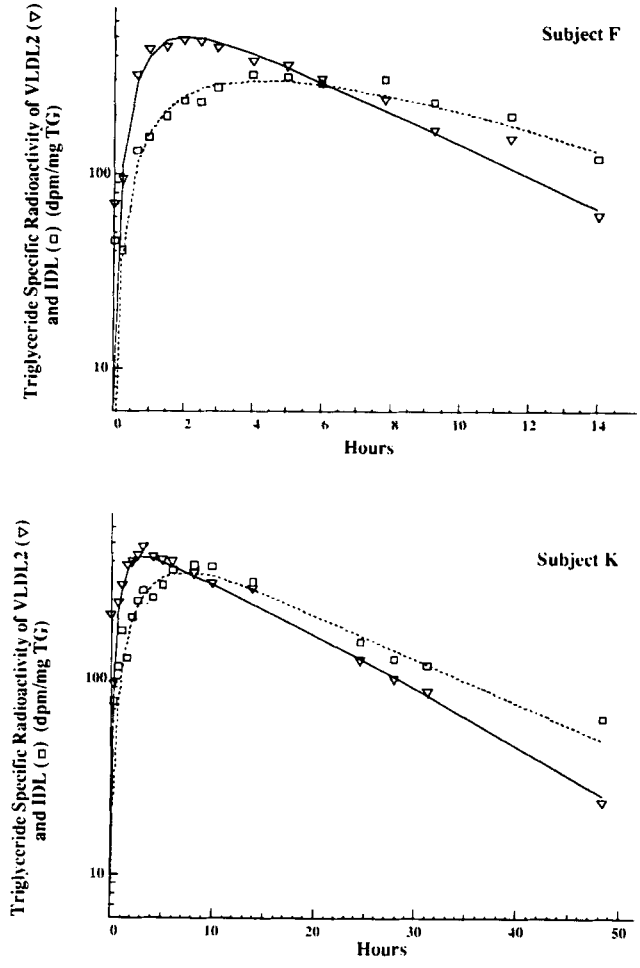

Fig. 8. Specific radioactivity curves of [^{3}H]triglyceride in unfractionated VLDL2 (▽) and IDL (□) for subjects F and K after i.v. injection of [2-^{3}H]glycerol. The symbols represent observations while the curves show the fits to the model (Fig. 9). The fits to the data were derived by coupling the ^{131}I-labeled apoB and triglyceride VLDL2 and IDL data.

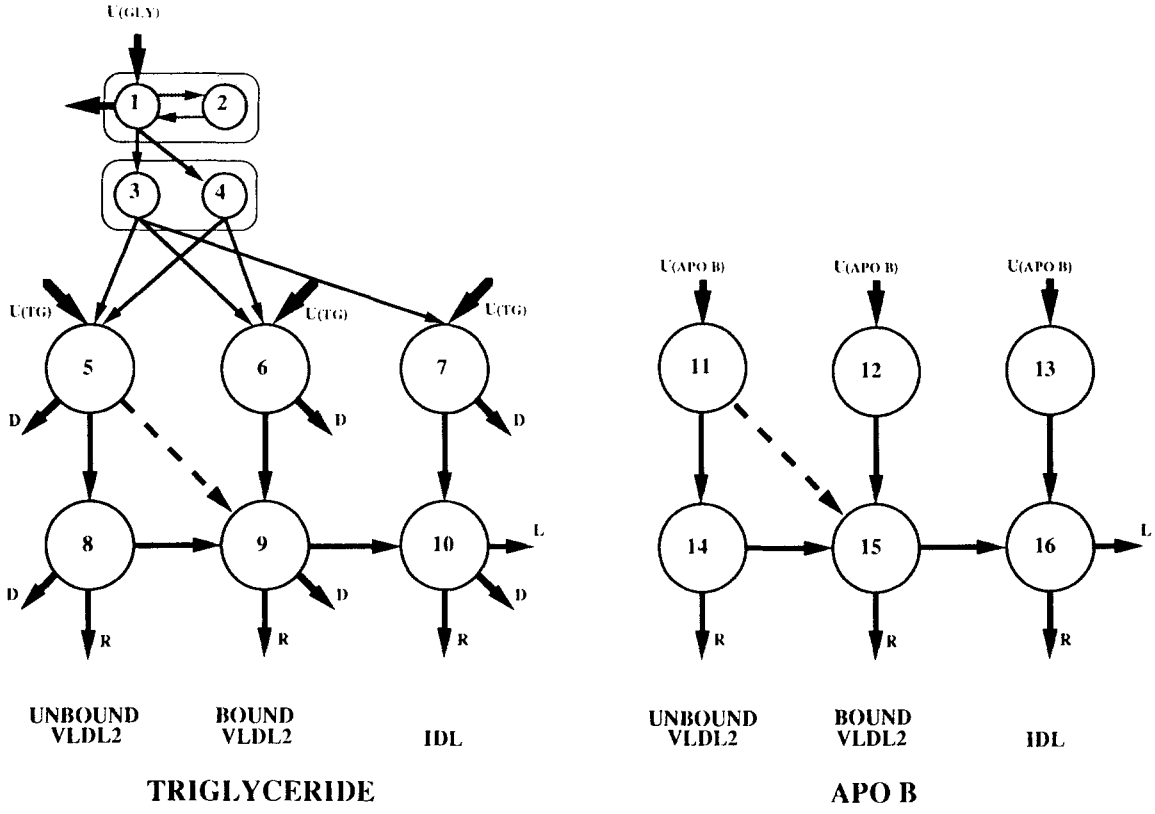

Fig. 9. VLDL2-triglyceride and -apoB model used for SAAM analysis of data. The model accounts for the kinetics of apoB and of triglyceride within the heparin-Sepharose unbound (unbound) and heparin-Sepharose bound (bound) VLDL2 fractions. Compartments 1 and 2 describe the kinetics of injected glycerol (assumed literature values). Compartments 3 and 4 represent the fast and slow hepatic glycerol to triglyceride conversion compartments, respectively. Compartments 5–10 and 11–16 were used to describe the observed kinetics of the triglyceride and apoB moieties, respectively, within the VLDL2 and IDL fractions. We have assumed that within the VLDL2 fractions, unbound and bound, with respect to both apoB and triglyceride there are particles that exhibit similar kinetic characteristics, hence the fractional turnover rates of compartments on the same level, i.e., 5, 6, 11, and 12, were equal. Implicit in this assumption is that the fractional turnover rate of apoB and of triglyceride compartments on the same level is the same. In the triglyceride model triglyceride is removed as a result of delipidation (D) from all compartments. In addition to this loss, triglyceride may be removed together with the particle from the remnant compartments (R). In the apoB model the direct removal of particles (R) from the remnant compartments may include uptake of particles and/or conversion to the IDL and subsequently LDL density range. Arrow L in both the triglyceride and apoB model represents the transport of particles from the IDL fraction to the LDL density range. In subject F, conversion of unbound VLDL particles to the bound fraction proceeded directly to the bound remnant compartment (dashed line) and not through the unbound remnant compartment (compartments 8 and 14).

remnant-like particles (C5 to C9, and C11 to C15); in this case the nascent-like particles dominate the kinetic behavior of apoB in the unbound VLDL fraction.

Two inputs from outside the system [$U_{(TG)}$] are shown entering C5 and C6 (Fig. 9), i.e., into the nascent VLDL-TG unbound and bound particles. Part of this input is probably from VLDL1, but we are unable to evaluate the extent of this contribution. Another part represents TG that is incorporated into nascent lipoproteins in the liver TG conversion system. In the rat model of Baker and Schotz (24) this is indicated by inputs into the liver TG compartments. However, in the human model of Zech et al. (6) this input is indicated as shown in Fig. 9. Although it may be misleading to show input into the plasma VLDL-TG compartments rather than into the liver where it actually enters, we have retained this convention along with the glycerol and liver TG conversion system based upon the data and model of Zech et al. (6).

Initially, each nascent compartment was subdivided into two compartments to depict a minimal delipidation chain; however, it was possible to account for the different residence times of VLDL-apoB and -TG by using the simpler model shown in Fig. 9. Thus, the four-compartment model consisting simply of nascent- and remnant-like particles linked as two- or three-compartment delipidation chains could account for the variety of kinetic behavior seen in the VLDL of our subjects. On the other hand, our data do not rule out the possibility that the VLDL2 (or VLDL1) delipidation chain is more complex. Ours is the simplest hypothetical working model consistent with the data and with published information regarding VLDL metabolism.

As with the VLDL fraction it was assumed that the IDL fraction was composed of a heterogeneous population of particles. Although the IDL apoB specific radioactivity data could be fit using a single compartment model, it was necessary to postulate the presence of two compartments in series, a minimal delipidation chain, to simultaneously account for the kinetics of the triglyceride in this fraction. As in the VLDL model, the turnover rate of the triglyceride-rich IDL particles (C7 and C13) was faster than that of the remnant IDL particles (C10 and C16). In addition, to account for the high and rapidly rising triglyceride specific radioactivity of the IDL fraction, a pathway from C3 directly to C7 was required (Fig. 9). The presence of a pathway from the more slowly turning over glycerol-to-triglyceride conversion compartment (C4) could not be determined. It was also hypothesized that, in addition to the direct input of triglyceride into the IDL fraction, there was input of apoB into compartment 13.

During model development, the apoB and triglyceride data were analyzed simultaneously. In addition, the residence times for apoB and triglyceride within a compartment were constrained to be equal; for example, the residence time of C5 (TG) was the same as that of C11 (apoB), thereby coupling the two moieties in the model. This point is discussed in more detail in a later section.

Impact of data parameters on model development

A brief summary of the relationships between the experimental data, particularly the slopes and intercepts of components of the VLDL specific radioactivity curves, and the structure of this portion of the model, including the logical basis for the initial estimates of the various fractional rate constants, follows.

The fast and slow compartments of the hepatic glycerol-to-triglyceride conversion subsystem for each subject were estimated from the falling slopes of the plasma VLDL2 unbound fraction's triglyceride specific radioactivity curve. In three subjects only the fast compartment could be identified, presumably because of the limited experimental period. Although the VLDL1 and VLDL2 models could not be integrated into one, different parameter values were used for the corresponding precursors of nascent VLDL1 and VLDL2 triglyceride to account for the differences in peak triglyceride specific radioactivities in VLDL1 and VLDL2, which, as noted earlier by Steiner and Ilse (25), suggests that the precursor of VLDL2 may have a higher specific radioactivity, and therefore that the precursors of VLDL1 and VLDL2 triglyceride are kinetically distinct. Theoretically, the maximum triglyceride specific radioactivities of the nascent VLDL1 and VLDL2 particles will equal those of their precursors at the time of maximal specific radioactivity, but that of VLDL2 would be lowered by the inflow of triglyceride of lower specific radioactivity coming from VLDL1, assuming that such a transformation occurs, and at a significant rate relative to the rate of direct inflow from the liver. In our model this transformation could not raise the maximal specific radioactivity of VLDL2 unless highly radioactive nascent VLDL1 particles were transformed to VLDL2 particles before mixing in the general circulation took place.

The rapidly rising portion of the plasma VLDL2 (and VLDL1) unbound fractions' triglyceride specific radioactivity curve was assumed to be dominated by the kinetic behavior of the nascent-like particles. However, this relationship is complex, due, in part, to the presence of remnant-like particles in the unbound fraction. This complexity is taken into account in the SAAM analysis. Given the additional assumptions described in the text, the unbound VLDL1 and VLDL2 triglyceride specific radioactivity data serve to define the residence times of the nascent-like particles within both the unbound and bound fractions, and therefore of both the apoB and the triglyceride moieties of the nascent particles (compartments 5, 6, 11, 12, Fig. 9). Evidence for the existence of nascent-like particles in the bound fraction is seen in the rapid rise of the bound triglyceride radioactivity curve; evidence of these particles in the apoB kinetics of the bound fraction, however, is not observed because of masking by the more slowly turning over remnant particles also in this fraction.

The unbound VLDL1 and VLDL2 apoB curves displayed the characteristic rapid slope expected for nascent-like particles in two subjects, F and H (VLDL1 only). However, by simulation analysis using the approach of Baker, Rostami, and Elovson (23), it could be shown that the presence of this rapid component, if it fed into a more slowly turning over remnant-like compartment in the same unbound fraction and assuming all particles had approximately the same initial specific radioactivity, would be masked by the kinetics of that compartment. We have assumed that a slowly turning over remnant-like compartment exists in both the unbound and bound fractions, but that in the subjects in which the rapid component appears in the unbound fraction the flow of radioactivity is from the unbound nascent (C5 and C11) to the bound remnant compartment (C9 and C15). In subjects in which the rapid component is not apparent in the unbound apoB specific radioactivity curve, we have assumed that the unbound nascent-like particle is converted to a more slowly turning over unbound remnant-like particle (C8 and C14), with a parallel flow occurring in the bound fraction (nascent to remnant). Some contamination by bound remnant-like particles of the unbound fraction was assumed to account for the tail component, such as that observed in subject F. In this subject, because the tail component described a population of particles that represented only a fraction of the bound fraction, the kinetics of the rapid component were visible, implying that these slowly turning over particles were not derived

from nascent-like unbound particles. When both a rapid and slow tail component appeared in the unbound apoB fraction, the slow component had the same slope as that of the bound remnant-like compartment (C9 and C15).

Although the apoB particles in the bound fraction often seemed to have a slower slope than the slow component of the unbound fraction, this occurred in cases in which a marked delay was observed in the bound fraction before the specific radioactivity fell. This delay as shown by Baker et al. (23) may be taken as evidence of the remnant-like particle's being derived from a similarly slowly turning over precursor compartment. We were able to show by simulation analysis that the slowly turning over remnant compartment of the bound fraction, assuming all particles had approximately the same initial specific radioactivity, would produce not only the observed delay, but would also distort the apparent "terminal" slope of the bound fraction, unless the experiment were to be extended beyond the times studied. Therefore, the apparently slower slopes of the bound fractions, in subjects H and K, were consistent with our assumption that remnant-like particles could appear in both unbound and bound fractions, that the remnants in both fractions had similar residence times, and that the unbound remnant feeds into the bound remnant fraction (to explain the delay seen only in the bound fraction).

In one subject, subject H, there was a slowly turning over tail evident in the VLDL2 triglyceride specific radioactivity curve. The kinetics of the tail were defined by the slow compartment in the glycerol-to-triglyceride conversion subsystem. Where no tail was present we were able to eliminate this compartment. Our model did not include a pathway for the recycling of [2-^{3}H]glycerol from VLDL2 to the glycerol compartment. Such recycling has been shown to be negligible (6).

Most models of VLDL triglyceride include a pronounced delay before newly synthesized triglyceride can be secreted into the circulation. However, we did not observe a delay before the rise of triglyceride specific radioactivity; therefore, no delay component appears in our model. The absence of a delay raised the possibility of contamination of VLDL-triglycerides by radiolabeled nontriglyceride material. However, we established by thin-layer chromatography that the early rise in radioactivity was not due to glycerol, phospholipid, or partial glycerides, and all radioactivity was shown to be associated with triglycerides.

Based upon observations made of subfractions of VLDL, the IDL section of the model developed in a way analogous to that of the VLDL model. Because IDL was not reinjected and because there were no heparin-Sepharose chromatographically separated IDL fractions, the amount of information describing the kinetics of the IDL fraction was less than that obtained for VLDL. Therefore, based upon the VLDL model, the assumption that the glycerol-to-triglyceride conversion process was rate-limiting, together with studies where labeled IDL-triglyceride was injected (26), it was hypothesized that, as with the VLDL fraction, the IDL fraction contained a population of particles that turned over more rapidly than the bulk of the particles within this fraction. Although the IDL apoB specific radioactivity data did not support the presence of such a group of particles, their presence would have been masked by the more slowly turning over IDL particles. Only with the rapid rise of the IDL triglyceride specific radioactivity curve was it evident that a population of rapidly turning over particles was present in the IDL fraction.

Additional assumptions

In the course of developing a model to account for both the apoB and triglyceride kinetics, the following additional assumptions were made. The first was that the residence times of apoB and triglyceride within a given compartment were the same; however, within each subfraction, represented by the sum of two compartments in series, the residence times for apoB and triglyceride differed according to Berman's definition (27). Thus, the model (Fig. 9) for the VLDL2 subsystem consists of two-compartment delipidation chains in which apoB moves from one compartment to the other, while only a fraction of the triglyceride is converted to the second compartment; the fraction not converted is assumed to be lost due to lipolysis (delipidation of the particle). It is conceivable, however, that the model we have presented is more complex, and that what we have identified as discrete compartments may, in fact, be the sum of a heterogeneous population of particles. Under these conditions we could not assume that the residence times of apoB and triglyceride within each (lumped) compartment would be the same.

The residence times of corresponding compartments that contain nascent- and remnant-like particles in the unbound and bound fractions were assumed to be equal. This assumption was consistent with the experimental observations as shown by multicompartmental analysis and as detailed in the text; however, this assumption, like most others that we have made, remains a working hypothesis until such time as all of the putative particles within each fraction can be analyzed as separate entities.

We assumed that, at zero time, the radioactivity within the reinjected VLDL was distributed in proportion to the apoB mass both in bound and unbound fractions, and in proportion to the pools of particles which existed within these fractions. Thus, apoB specific radioactivity of the particles within each fraction, unbound or bound, was assumed to be equal. However, we observed that the apoB specific radioactivities of the bound and unbound fractions of the recipient subjects (i.e., after mixing of the injected tracer with the endogenous pools) were not always

equal at zero time. We have assumed that these initial differences, also observed by Nestel et al. (8), reflected a change in the distribution of bound and unbound apoB pools within the subject between the time the tracer was prepared and the time it was reinjected. This difference in the initial specific radioactivities of the unbound and bound fractions was taken into account during the modeling of the data. An alternative explanation, discussed above, is that these differences may be due to the nonuniform labeling of apoB.

Our final model required the assumption that newly secreted VLDL particles are found in both unbound and bound fractions. This assumption, which contrasted to that made in designing our experiment, was consistent with an earlier observation of Nestel et al. (8) that showed that, after reinjection of ^{125}I-labeled unbound apoB, the initial specific radioactivity of the bound fraction, which would be expected to be zero, was greater than this but less than that of the unbound fraction. This observation supports the existence of two populations of particles in the bound fraction, one that equilibrates rapidly with the unbound particles, and one that does not. Most of the apoB mass of the bound fraction is associated with the slowly turning over remnant-like particles, which are not involved in a rapid interconversion process.

In the case of subject J, who received [2-^{3}H]glycerol only, we assumed apoB parameters based on the data of subject K whose lipoprotein profile and triglyceride specific radioactivity data were comparable to those of subject J.

Modeling results

Table 5 summarizes the fractional turnover rates for each of the compartments shown in the VLDL2 model of Fig. 9, but expressed in terms of nascent-level and remnant-level compartments, as defined in Table 5. This simplification is possible because of our assumptions that corresponding unbound and bound particles have equal residence times at any level and that triglycerides and apoB also have equal residence times or turnover times at the same levels. As shown in Table 5, the nascent-level compartments in VLDL2 turn over at a rate of approximately 1 per hour in each of the three hyperlipidemic subjects. The turnover rate of the remnant-level compartments is, however, much slower, between 0.1 and 0.2 per hour. Only in subject F was it possible to observe the rapid kinetics of the putative nascent-level compartment, predicted by the triglyceride data, in the VLDL2 apoB data. In this subject the slope of the fast component of the unbound apoB disappearance curve was equal to that of the upswing of the triglyceride specific radioactivity curve. In all subjects, however, even when the fast slope of the unbound apoB curve was not observed and was assumed to be masked by a more slowly turning over product, the turnover rate of the nascent-level compartments was defined by the rate of rise of the triglyceride specific radioactivity curve.

TABLE 5. Fractional turnover rates of nascent- (N-) and remnant- (R-) level compartments in VLDL2[a]

	N-Level	R-Level
	h^{-1}	
F	1.31 (0.04)	0.21 (0.01)
K	1.22 (0.11)	0.09 (0.02)
H	1.01 (0.09)	0.18 (0.01)

Values in parentheses are ± SD.
[a]The values in this table represent the sum of the exiting L(i,j) of the compartments on levels N and R in the VLDL2 model (see Fig. 9).

Examination of the distribution of VLDL2 apoB between the nascent- and remnant-level compartments (**Table 6**) clearly shows that more than 85% of VLDL apoB, and hence lipoprotein particles, was associated with the slowly turning over remnant-level VLDL2 fraction. In contrast, in three subjects, most of the VLDL2 triglyceride (63–75%) was associated with the nascent-level compartments (Table 6).

The triglyceride/apoB ratios, calculated on the basis of the kinetic analyses of the unbound and bound VLDL triglyceride and apoB fractions and the measured VLDL2 pool sizes, are shown in Table 6. As noted in the footnote to Table 6, the directly measured TG/apoB ratios presented in Table 3 correspond to the weighted mean of the values calculated in the SAAM analysis. The triglyceride/apoB ratios of compartments on the same level, i.e., nascent- or remnant-level, were assumed to be equal. At the nascent level of the model most particles are found in the unbound fraction, whereas most remnant-like particles were in the bound fraction. This distribution of particles allows the TG/apoB ratio of unbound and bound fractions to differ even though at any level the ratio is the same for bound and unbound compartments. The triglyceride/apoB ratio of the remnant-level compartments was an order of magnitude below that of the nascent-level compartments, thereby defining the extent of the delipidation that occurred in this transformation.

VLDL2 apoB and triglyceride fractional catabolic rates (FCR) and production rates were determined for each subject (**Table 7**). ApoB production rates in VLDL2 were comparable to those which have been observed by other workers (28–30). Despite our attempt to do so, we were unable to determine the relative input of apoB from the liver into the plasma VLDL2 fraction (direct input in contrast to formation from VLDL1), for reasons noted above. Therefore, the production rates shown in Table 7 describe total apoB production in the VLDL2 fraction. In

contrast to the apparently normal production rates for VLDL2 apoB, triglyceride production rates and FCR were higher (2–6 times) than those measured by other workers for comparable subjects (11, 28, 31). Comparison of VLDL2 apoB production rates with those calculated for IDL (**Table 8**) reveal that in subjects F and H approximately 50% of VLDL2 apoB was not converted to IDL and was presumably removed directly from circulation. In contrast, IDL triglyceride production rates show that the amount of triglyceride converted to the IDL fraction from VLDL2 was negligible and that more than 70% of triglyceride production through IDL was derived directly from non-VLDL2 sources, presumably from the liver. The contribution to IDL triglyceride production from VLDL1 directly into IDL could not be determined.

TABLE 7. VLDL2 apoB and triglyceride production and fractional catabolic rates

	ApoB			Triglyceride		
	Pool Size	*Production*	*FCR*	*Pool Size*	*Production*	*FCR*
	mg	*mg/kg/d*	h^{-1}	*mg*	*mg/kg/d*	h^{-1}
F	455	20.3 (0.4)	0.18 (0.01)	5592	1356 (65)	0.99 (0.05)
K	622	10.1 (0.2)	0.05 (0.01)	6528	931 (213)	0.47 (0.11)
H	756	29.1 (1.2)	0.11 (0.01)	4360	909 (143)	0.61 (0.09)
J	694	n.d.[a]	n.d.	8011	1862[b] (230)	1.09[b] (0.13)

Values in parentheses are ± SD.
[a]Not determined.
[b]Values determined using apoB parameters derived from fitting subject K.

DISCUSSION

The analysis of the data presented here represents a new approach to the study of VLDL apoB and VLDL triglyceride production and metabolism in four hypertriglyceridemic subjects. This presentation primarily deals with the turnover of the apoB and triglyceride moieties of circulating nascent VLDL1 and VLDL2 particles, the conversion of nascent to remnant-like VLDL particles within the VLDL1 and VLDL2 particle populations, and the complex relationships among hepatic precursors of nascent VLDL1 and VLDL2. In addition, rates of VLDL2 removal by transformation to IDL and of direct input of apoB and triglyceride into IDL in these subjects is presented.

TABLE 6. Distribution of apoB, triglyceride and the triglyceride/apoB ratio of N- and R-level compartments within VLDL2[a]

	Level	ApoB	Triglyceride	Triglyceride/ApoB
		%[b]	%[b]	mg/mg
F	N	13.9	75.2	66.7
	R	86.1	24.8	8.3
K	N	4.7	38.4	91.8
	R	95.3	61.6	6.8
H	N	10.1	64.6	35.8
	R	89.9	35.4	2.3
J[c]	N	5.6	62.5	129.4
	R	94.4	37.5	4.6

[a]The triglyceride/apoB ratios of the unfractionated VLDL2 fraction shown in Table 3 are the weighted average of the ratios presented in this Table.
[b]Expressed as a percentage of the total mass in VLDL2 associated with the nascent- (N-) and remnant- (R-) level compartments, such that % in N- and % in R-level = 100%.
[c]Values based upon apoB parameters derived from fitting subject K.

Our experimental design was based on several major assumptions, each of which had a major impact on our analysis, provided fresh insights, and indicated new directions that might be taken in future kinetic studies of VLDL metabolism in humans. First, we assumed that the hepatic triglyceride precursor compartments of nascent VLDL particles are rate-limiting with respect to VLDL triglyceride kinetics.[4] Thus, we considered the slope of the rapid upswing of the VLDL triglyceride specific radioactivity curve to be influenced primarily by the turnover rate of newly secreted nascent plasma VLDL particles, rather than by that of their precursor hepatic triglyceride compartment. From this it follows that the hepatic triglyceride pools turn over slowly, at rates approximating the declining portion of the VLDL triglyceride specific activity curve after it has reached its maximum, as in the rat liver-plasma triglyceride model of Baker and Schotz (24).

Second, we assumed that the rate of large VLDL1 transformation to smaller VLDL2 particles could be estimated by the injection of homologous, doubly labeled VLDL1 and VLDL2 apoB tracers into each subject and analyzing nascent- and remnant-rich particles within each of the VLDL fractions. Although theoretically a valid approach (3), we were unable to integrate the combined VLDL1 and VLDL2 data into our model. After the injection of ^{125}I-labeled VLDL1 in each of three hypertriglyceridemic subjects, there was an almost immediate transformation of 50–90% of the tracer into both un-

[4]This assumption has not been made in earlier studies of VLDL-triglyceride turnover in humans (6, 32), but it has been found to be the case in all other animal species that have been studied in detail (24, 33–38). Studies from Steiner's laboratory, which showed striking similarities between VLDL triglyceride kinetic behavior in humans (39) and in dogs (25), in which the liver triglyceride precursor compartments are known to be rate-limiting (36), strengthened this assumption.

TABLE 8. IDL apoB and triglyceride production and fractional catabolic rates

	ApoB				Triglyceride			
	Pool Size	Total Prodn.	Direct Prodn.	FCR	Pool Size	Total Prodn.	Direct Prodn.	FCR
	mg	*mg/kg/d*		h^{-1}	*mg*	*mg/kg/d*		h^{-1}
F	232	11.0 (0.8)	1.4 (0.4)	0.19 (0.01)	478	40.6 (2.8)	36.9 (2.9)	0.34 (0.02)
K	348	10.1 (0.1)	0.9 (0.2)	0.07 (0.001)	1020	38.5 (7.3)	32.5 (8.1)	0.12 (0.03)
H	300	12.2 (1.0)	3.2 (0.6)	0.12 (0.01)	644	32.6 (1.9)	28.5 (2.3)	0.15 (0.01)
J	216	n.d.[a]	n.d.	n.d.	551	32.7[b] (3.9)	23.3 (3.7)	0.22 (0.03)

Values in parentheses are ± SD.
[a]Not determined.
[b]Values determined using apoB parameters derived from fitting subject K.

bound and bound VLDL2 fractions. This obscured the kinetics of any apoB-containing particles derived from VLDL1, assuming that they were being transformed at rates comparable to those of VLDL2 turnover, to smaller VLDL2 particles. The rapid conversion of VLDL1 to VLDL2, which was evident within 3 min after injection, could have been an artifact of VLDL1 ultracentrifugal isolation and labeling. However, it was not seen when VLDL1 particles were labeled, incubated with plasma, and then separated again into VLDL1 and VLDL2 fractions; the radioactivity remained with the VLDL1 particles. Therefore, in each of the hypertriglyceridemic subjects studied, the VLDL1 particles were being transformed in vivo into VLDL2 particles by a very rapid process that may or may not be physiological. It is conceivable that, during isolation of VLDL1 for labeling, apolipoproteins were lost from some of the VLDL1 particles, and that upon injection of the labeled VLDL1 a fraction of the tracer was rapidly remodeled resulting in an increase in its density. In addition to this explanation, it may be that in our subjects the VLDL particles were concentrated at the border of the VLDL1 and VLDL2 density cut. With subtle changes, such as those described above, a small shift in density could move the VLDL1 particles into the VLDL2 fraction. If this is the explanation then we would expect the kinetics of the VLDL1 and VLDL2 fractions to be similar; this is, in fact, what we observed. Nevertheless, we were able to see from the incorporation of [2-^{3}H]glycerol into triglycerides of the unbound and bound VLDL1 fractions that nascent VLDL1 particles were being introduced into the circulation at rates comparable to the formation of nascent VLDL2 particles. Furthermore, nascent particles appeared almost simultaneously in both the unbound and bound fractions of VLDL1, corroborating our conclusion (see below) that heparin-Sepharose chromatography was not separating the VLDL particles cleanly into nascent and remnant (i.e., precursor and product) fractions.

Third, we assumed initially that heparin-Sepharose affinity chromatography would separate VLDL particles into nascent- and remnant-rich VLDL particles, found in the unbound and bound fraction, respectively, based upon the earlier work of Nestel et al. (8), reanalyzed by the theoretical approach of Baker et al.[3] This reanalysis showed that labeled apoB in the unbound and bound particles often exhibited the kinetic relationship expected for precursor (nascent) and product (remnant) compartments. However, while the apoB kinetic data in the present study were consistent with our assumption that the unbound and bound VLDL particles behaved as precursor and product, respectively, the triglyceride specific activity data after injecting tracer glycerol were not. Nascent particles containing newly synthesized triglyceride appeared simultaneously in unbound and bound fractions.

Although we observed that bound VLDL remnant-like particles were converted to IDL, we cannot rule out the presence in the former of some rapidly turning over, largely delipidated VLDL remnants that might be removed by the liver. Such remnant particles would have to be present in low concentration and their kinetic behavior be masked by that of the more slowly turning over bound remnant-like particles, from which they would be derived. The technique that we have used clearly does not allow us to characterize a rapidly turning over VLDL remnant fraction, should such a fraction exist in these subjects.

The appearance of newly secreted VLDL in both the unbound and bound fractions is consistent with many diverse studies dealing with the chemical characterization of VLDL particles isolated by heparin-Sepharose affinity columns, which divide particles into apoE-enriched (8, 13, 40, 41) and either apoE-free (40, 41) or apoE-poor (8, 13) fractions, depending upon the conditions used. The presence of nascent-like particles in both fractions is also consistent with the kinetic behavior of the separated particles in humans (8), pigs (13), and rabbits (41), with the relation of apolipoprotein composition to binding (42, 43), and with the continuous metabolic remodeling of nascent and more mature VLDL particles, especially with respect to the relative apoE and apoC concentrations (43–50). Based upon this literature we were able to fit our data to the model by assuming *1*) that particles secreted from the liver initially have a high apoE/apoC ratio (thus, bindable to the apoB/E or E receptors in liver and other tissues); and *2*) are rapidly remodeled within plasma to acquire apoC and/or lose apoE, decreasing the apoE/apoC ratio and rendering them less bindable. Evidence for this rapid remodeling process comes from the earlier studies of Nestel et al. (8) and from the different relationships seen between VLDL apoB and triglyceride

kinetics in the unbound and bound fractions observed in these studies. As these particles are delipidated, decreasing their requirement for apoC, there is a loss of apoC from the particle, raising the apoE/apoC ratio, again making them bindable and prone to removal from the circulation. The rate at which these bound, partially delipidated particles are metabolized, however, is slower than that of the more nascent-like particles which are present in both the unbound and bound fractions. Newly synthesized triglyceride will, therefore, be found in both bound and unbound particles shortly after the entry of nascent VLDL into the circulation.

One experimental aim was to see whether labeled apoB in the heparin-Sepharose nascent-rich unbound VLDL1 and VLDL2 fractions of at least some of the hypertriglyceridemic subjects would display the rapid FCR predicted for nascent particles if the liver TG precursor compartment were rate-limiting. Reanalysis of the data of Nestel et al. (8) had indicated that such a rapid component might be found in about a third of the subjects studied. We corroborated these findings and have tried to explain the observation that the rapidly turning over apoB component was only observed in the unbound and not in the bound VLDL fraction, and then in only some of the subjects, by hypothesizing that in the bound VLDL fraction the rapid component is masked by the presence of slowly turning over, remnant-like particles that are derived from the nascent-like precursors, but is only masked in the unbound fraction if the nascent-like unbound particle forms a slowly turning over remnant-like particle that is also recovered in the unbound fraction.

Although the subjects studied showed marked variations in the distribution of apoB and triglyceride among the various fractions, in three subjects most lipoprotein particles were found within the VLDL2 fraction, and in all cases the bound VLDL2 contained more particles than the unbound fraction. The VLDL2 had a higher cholesterol/triglyceride ratio and a lower triglyceride/apoB ratio than those in the VLDL1 fraction. This suggests that the VLDL2 fraction contained more remnant-like particles. However, as noted above, analysis of the VLDL2 triglyceride kinetics indicated that this fraction also contained a large number of nonremnant particles. This was further evidenced by the higher triglyceride/apoB ratio in the unbound VLDL2 than in the bound VLDL1 fractions.

Despite these considerable problems of heterogeneity, we have been able to incorporate into a single model the kinetics of VLDL triglyceride and of VLDL apoB observed within the four subfractions (VLDL1 and VLDL2, unbound and bound particles). Although relatively complex, we believe that this model represents the simplest structure that is consistent with the data and the relationships we have observed between the unbound and bound apoB and triglyceride moieties. The model has three main features; two compartments of unbound-bound (nascent-like) particles, two parallel delipidation pathways, and a shared bound (remnant-like) pool. The technique of modeling both moieties concurrently has been undertaken by relatively few workers (5, 51, 52), despite the insights and benefits that can be obtained. Furthermore, the rising slope of the VLDL-triglyceride specific radioactivity curve has not previously been used to provide information about the turnover rate of the nascent plasma VLDL particles in human subjects, an approach used in earlier quantitative studies of plasma and liver triglyceride turnover in animals (24, 53, 54).

The data for the apoB kinetics display the features reported recently by others (3, 5), although our analysis of the separated bound and unbound fractions has provided additional insight into the complexity of the catabolic processes. Whereas the fractional removal rates of whole VLDL1 and VLDL2 are relatively slow as observed by others in hypertriglyceridemic subjects (3, 5, 31), there is a rapidly catabolized minor fraction represented by a proportion of the unbound particles, especially within VLDL1 (Table 4). Other workers have postulated the existence of such a pool of rapidly removable larger VLDL particles (5). As discussed later, this has influenced our interpretation of the triglyceride data.

The input of apoB and triglyceride was, however, not only confined to the VLDL2 density range. The model calculates that for the IDL density range there is also direct input, and although the absolute amounts of direct input are low compared to that into the VLDL2 fraction they represent a significant proportion of the transport through the IDL. This would, therefore, suggest that the liver is capable of secreting lipoproteins of different size which need not necessarily be secreted into the VLDL1 density range. An alternative explanation may be that partly catabolized particles, as they pass through the hepatic circulation, become re-enriched with newly synthesized triglyceride. However, as noted above, the use of fixed anglehead rotors, as used in our studies, may lead to the incomplete separation of IDL from the smallest VLDL (3). Conversely the VLDL tail may, in part, reflect the inclusion of slowly turning over IDL.

Multiple inputs and exits for VLDL particles of different sizes have been reported in all recently modeled systems of VLDL metabolism in man. Although the concept of direct secretion of smaller VLDL particles has been criticized on the basis that a rapidly turning over precursor particle can be missed by exogenous labeling techniques (5), this should not apply to the analysis of endogenously labeled lipoproteins. It is therefore noteworthy that Fisher et al. (4) using [^{3}H]leucine as a precursor label for apoB, reported rapid, simultaneous rates of labeling of large and small VLDL. Furthermore, they noted major biosynthetic inputs even into IDL in hypertriglyceridemic subjects (4). Eaton et al. (2) who used [^{75}Se]selenomethionine as the precursor label

observed major inputs into both the initial and final VLDL pools (within a four-pool cascade) in both hypertriglyceridemic and normolipidemic subjects. A massive input into the largest initial kinetic pool of the VLDL was a hallmark of hypertriglyceridemia (2). This is highly relevant to the possible failure of models based on exogenously labeled VLDL to identify this major influx of large VLDL, especially since Eaton et al. (2) had also found that these particles were least likely to be catabolized to IDL.

Such findings are nevertheless in line with the models developed by Beltz et al. (5) and by Packard et al. (3) who integrated data from the kinetics of several exogenously labeled lipoprotein species. Both models consider multiple inputs at the beginning or near the end of the VLDL delipidation cascade, although the conclusion reached in one study was that a variable and flexible number of VLDL pools could explain the data without involving a need for multiple inputs (5). However, Packard et al. (3) drew attention to the metabolic channeling of particles within the spectrum of smaller VLDL, with those derived from the catabolism of larger VLDL having a different fate from those newly secreted; a larger fraction of the latter were destined for conversion to LDL.

Our data have also described more fully the delipidation that converts nascent triglyceride-rich VLDL into triglyceride-depleted remnants. The extended plateau of the bound fraction reflected the long delipidation process which did not apply to the unbound fraction. This was also observed in the bound apoB fractions which showed a pronounced delay prior to the fall in specific radioactivity. ApoB turnover experiments, which use exogenously labeled VLDL, do not, in general, show this delipidation process clearly unless the VLDL have been extensively subfractionated or early serial samples are obtained.

The higher triglyceride/apoB ratio in the unbound VLDL2 fraction than in the bound VLDL1 had already suggested that independent input of new triglyceride into the VLDL2 fraction was likely. Nevertheless, the ratios in the corresponding unbound fractions showed these to be higher in VLDL1. The liver may therefore be secreting at least two different types of particles, the VLDL1 being more triglyceride-enriched than the VLDL2. Analysis of the kinetics of the most nascent triglyceride pools in the model for both the VLDL1 and VLDL2 fractions reveals that their respective hepatic assembly processes may differ. Estimates of the VLDL precursor specific radioactivities, determined by simulation analysis of the triglyceride precursor pools, showed that in two of the four subjects the precursor triglyceride pool for VLDL2 had approximately ten times the activity of the VLDL1 precursor. Streja, Kellai, and Steiner (39) and Steiner and Reardon (52) had also observed that the smaller VLDL attained a greater specific radioactivity than did the larger VLDL, an observation that we have confirmed.

In addition to the TG/apoB ratio of the unbound VLDL2 being greater than that of the bound VLDL1, the model predicted that within each fraction, unbound- and bound-VLDL and IDL, there were particles with high TG/apoB ratios. Excluding subject J, the TG/apoB ratios of the nascent-level compartments in VLDL2 were of the order of 100 and up to 36 for IDL. TG/apoB ratios such as these are greater than those generally observed in VLDL and IDL fractions. If particles with such high TG/apoB ratios are to be isolated in their respective density classes, clearly there must be other apolipoproteins associated with the more TG-rich particles that increase their density. In most previous studies workers have subfractionated lipoproteins according to density and have not isolated them on the basis of the particles' metabolic properties, hence most fractions are likely to comprise a mixture of nascent- and remnant-like particles. When, however, detailed fractionation of lipoproteins by a method such as heparin-Sepharose affinity chromatography is undertaken, large variations in TG/apoB ratios approaching those we have predicted are observed (55, 56), especially in the case of Winkler and Marsh (57) where nascent triglyceride-rich, apoB-poor particles were found in the HDL fraction.

The absolute production rates for VLDL triglyceride obtained in these subjects with our model are considerably higher than those reported by others in type IV hyperlipoproteinemia. Published production rates for triglyceride vary considerably, depending on the method by which the values have been calculated (28). Many values, for the $d < 1.006$ g/ml ($S_f > 20$), are around 200–400 mg/kg per day (11, 28, 31, 58) although Boberg et al. (59) reported an average of 983 mg/kg per day for hypertriglyceridemic subjects. Our values, for VLDL2 triglyceride alone, are within the range of those obtained by others measuring whole VLDL triglyceride production. This, in addition to VLDL1 triglyceride production (which was not calculated in the present experiment for reasons previously discussed), would result in total VLDL-triglyceride production values several to many times those calculated by others. Clearly this suggests that VLDL triglyceride production may be greater than has been calculated previously. The assumption that triglyceride turnover in the liver is rate-limiting with respect to plasma triglyceride, coupled with the observation of a rapidly turning over population of particles, which contains the greater proportion of the triglyceride mass within each VLDL fraction, account for the high triglyceride production values. A comparison of VLDL2-triglyceride production rates with those determined using the Zech et al. model (6), where it is assumed that the liver is not rate limiting, showed that production rates in our subjects were one-half to one-eighth those determined using the present model.

The subjects that were studied in these experiments,

while all showing the type IV hyperlipoproteinemia phenotype, were not identical, this being reflected in their apoB and triglyceride kinetics. Two subjects, H and F, who had similar lipoprotein profiles, displayed substantial shunting of material, presumably back to the liver, direct input of both apoB and triglyceride into VLDL2 and IDL, and high levels of total triglyceride production. Subject K, however, whose VLDL mass was mostly in the VLDL1 density range, displayed a different pattern of apoB and triglyceride kinetics. Possibly, the very low VLDL2 FCR of this subject may be accounted for by the presence of chylomicron remnants that have been found throughout the lipoprotein spectrum (60). Chylomicron remnants within this fraction have been shown to be catabolized slowly in type 5 hyperlipoproteinemic subjects (61). Appendix Tables 1 and 2 follow on page 762.

We kindly acknowledge the expert assistance of Patricia Nugent and Liz Faehse. This research was supported in part by a grant from the National Heart Foundation of Australia. N. Baker was supported in part by National Cancer Institute Grant CA-15813.

Manuscript received 11 January 1988, in revised form 27 December 1989, in re-revised form 19 October 1990, and in re-re-revised form 22 January 1991.

REFERENCES

1. Grundy, S. M. 1984. Pathogenesis of hyperlipoproteinemia. *J. Lipid Res.* **25:** 1611–1618.
2. Eaton, R. P., R. C. Allen, and D. S. Schade. 1983. Overproduction of a kinetic subclass of VLDL-apoB and direct catabolism of VLDL-apoB in human endogenous hypertriglyceridemia: an analytical model solution of tracer data. *J. Lipid Res.* **24:** 1291–1303.
3. Packard, C. J., A. Munro, A. R. Lorimer, A. M. Gotto, and J. Shepherd. 1984. Metabolism of apolipoprotein B in large triglyceride-rich very low density lipoproteins of normal and hypertriglyceridemic subjects. *J. Clin. Invest.* **74:** 2178–2192.
4. Fisher, W. R., L. A. Zech, P. Bardalaye, G. Warmke, and M. Berman. 1980. The metabolism of apolipoprotein B in subjects with hypertriglyceridemia and polydisperse LDL. *J. Lipid Res.* **21:** 760–774.
5. Beltz, W. F., Y. A. Kesaniemi, B. V. Howard, and S. M. Grundy. 1985. Development of an integrated model for analysis of the kinetics of apolipoprotein B in plasma very low density lipoproteins, intermediate density lipoproteins, and low density lipoproteins. *J. Clin. Invest.* **76:** 575–585.
6. Zech, L. A., S. M. Grundy, D. Steinberg, and M. Berman. 1979. Kinetic model for production and metabolism of very low density lipoprotein triglycerides. *J. Clin. Invest.* **63:** 1262–1273.
7. Berman, M., H. Hall, R. I. Levy, S. Eisenberg, D. W. Bilheimer, R. D. Phair, and R. H. Goebel. 1978. Metabolism of apoB and apoC lipoproteins in man: kinetic studies in normal and hyperlipoproteinemic subjects. *J. Lipid Res.* **19:** 38–56.
8. Nestel, P. J., T. Billington, N. Tada, P. Nugent, and N. H. Fidge. 1983. Heterogeneity of very low density lipoprotein metabolism in hyperlipidemic subjects. *Metabolism.* **32:** 810–817.
9. McFarlane, A. S. 1958. Efficient trace-labelling of proteins with iodine. *Nature.* **182:** 53–57.
10. Fidge, N. H., and P. Poulis. 1974. Studies on the radioiodination of VLDL obtained from different mammalian species. *Clin. Chim. Acta.* **52:** 15–26.
11. Grundy, S. M., H. Y. Mok, L. Zech, D. Steinberg, and M. Berman. 1979. Transport of very low density lipoprotein triglycerides in varying degrees of obesity and hypertriglyceridemia. *J. Clin. Invest.* **63:** 1274–1283.
12. Shelburne, F. A., and S. H. Quarfordt. 1977. The interaction of heparin with an apoprotein of human very low density lipoprotein. *J. Clin. Invest.* **60:** 944–950.
13. Huff, M. W., and D. E. Telford. 1984. Characterization and metabolic fate of two very-low-density lipoprotein subfractions separated by heparin-Sepharose chromatography. *Biochim. Biophys. Acta.* **796:** 251–261.
14. Methods N24A and N78 of Technicon Autoanalyzers. Technicon Inst. Corp. Tarrytown, NY.
15. Reardon, M. F., M. E. Poapst, K. D. Uffelman, and G. Steiner. 1981. Improved method for quantitation of B apoprotein in plasma lipoproteins by electroimmunoassay. *Clin. Chem.* **27:** 892–895.
16. Egusa, G., D. Brady, S. M. Grundy, and B. V. Howard. 1983. Isopropanol precipitation method for the determination of apoB specific activity and plasma concentrations during metabolic studies of VLDL and LDL apoB. *J. Lipid Res.* **24:** 1261–1267.
17. Dole, V. P., and H. Meinertz. 1960. Microdetermination of long-chain fatty acids in plasma and tissues. *J. Biol. Chem.* **235:** 2595–2599.
18. Neri, B. P., and C. S. Frings. 1973. Improved method for determination of triglycerides in serum. *Clin. Chem.* **19:** 1201–1202.
19. Berman, M., and M. F. Weiss. 1978. SAAM Manual. DHEW Publ. No. (NIH) 78-180. 1–196.
20. Boston, R. C., P. C. Greif, and M. Berman. 1981. Conversational SAAM—an interactive program for kinetic analysis of biological systems. *Comput. Programs Biomed.* **13:** 111–119.
21. Musliner, T. A., C. Giotas, and R. M. Krauss. 1986. Presence of multiple subpopulations of lipoproteins of intermediate density in normal subjects. *Arteriosclerosis.* **6:** 79–87.
22. Ramakrishnan, R., Y. Arad, S. Wong, and H. N. Ginsberg. 1990. Nonuniform radiolabeling of VLDL apolipoprotein B: implications for the analysis of studies of the kinetics of the metabolism of lipoproteins containing apolipoprotein B. *J. Lipid Res.* **31:** 1031–1042.
23. Baker, N., H. J. Rostami, and J. Elovson. 1983. Nascent and remnant lipoprotein turnover in rats: experimental design and simulation. *Am. J. Physiol.* **245:** R386–R395.
24. Baker, N., and M. C. Schotz. 1964. Use of multicompartmental models to measure rates of triglyceride metabolism in rats. *J. Lipid Res.* **5:** 188–197.
25. Steiner, G., and W. K. Ilse. 1981. Heterogeneity of VLDL triglyceride production by the liver and intestine. *Can. J. Biochem.* **59:** 637–641.
26. Malmendier, C., and M. Berman. 1978. Endogenously labeled low density lipoprotein triglyceride and apoprotein B kinetics. *J. Lipid Res.* **19:** 978–984.
27. Berman, M. 1979. Kinetic analysis of turnover data. *Prog. Biochem. Pharmacol.* **15:** 67–108.
28. Sigurdsson, G., A. Nicoll, and B. Lewis. 1976. Metabolism of very low density lipoprotein in hypertriglyceridemia: studies of apolipoprotein B kinetics in man. *Eur. J. Clin. Invest.* **6:** 167–177.
29. Reardon, M. F., N. H. Fidge, and P. J. Nestel. 1978. Cata-

bolism of very low density lipoprotein B apoprotein in man. *J. Clin. Invest.* **61:** 850–860.
30. Janus, E. D., A. M. Nicoll, P. R. Turner, P. Magill, and B. Lewis. 1980. Kinetic bases of the primary hyperlipidemias: studies of apolipoprotein B turnover in genetically defined subjects. *Eur. J. Clin. Invest.* **10:** 161–172.
31. Beil, U., S. M. Grundy, J. R. Crouse, and L. Zech. 1982. Triglyceride and cholesterol metabolism in primary hypertriglyceridemia. *Arteriosclerosis.* **2:** 44–57.
32. Farquhar, J. W., R. C. Gross, R. M. Wagner, and G. M. Reaven. 1965. Validation of an incompletely coupled two-compartment nonrecycling catenary model for turnover of liver and plasma triglyceride in man. *J. Lipid Res.* **6:** 119–134.
33. Laurell, S. 1959. Recycling of intravenously injected palmitic acid-1-C^{14} as esterified fatty acid in the plasma of rats and turnover rate of plasma triglycerides. *Acta Physiol Scand.* **47:** 218–232.
34. Havel, R. J., J. M. Felts, and C. M. Van Duyne. 1962. Formation and fate of endogenous triglycerides in blood plasma of rabbits. *J. Lipid Res.* **3:** 297–308.
35. Havel, R. J. 1968. Triglyceride and very low density lipoprotein turnover. *In* Proceedings of the Deuel Conference of Lipids. Cowgil, Estrich and Wood, editors. US Government Printing Office. 115–130.
36. Gross, R. C., E. H. Eigenbrodt, and J. W. Farquhar. 1967. Endogenous triglyceride turnover in liver and plasma of the dog. *J. Lipid Res.* **8:** 114–125.
37. Lipkin, E. W., C. Cooper, and R. A. Shipley. 1978. The contribution of serum triacylglycerol in hepatic triacylglycerol turnover in the starved rat. *Biochem. J.* **172:** 205–218.
38. Hannan, S. F., N. Baker, H. Rostami, K. Lewis, and P. J. Scott. 1980. Very low density lipoprotein metabolism in domestic pigs. *Atherosclerosis.* **37:** 55–68.
39. Streja, D., M. A. Kallai, and G. Steiner. 1977. The metabolic heterogeneity of human very low density lipoprotein triglyceride. *Metabolism.* **26:** 1333–1344.
40. Fielding, P. E., and C. J. Fielding. 1986. An apo-E-free very low density lipoprotein enriched in phosphatidylethanolamine in human plasma. *J. Biol. Chem.* **261:** 5233–5236.
41. Yamada, N., D. M. Shames, J. B. Stoudemire, and R. J. Havel. 1986. Metabolism of lipoproteins containing apolipoprotein B-100 in blood plasma of rabbits: heterogeneity related to the presence of apolipoprotein E. *Proc. Natl. Acad. Sci. USA.* **83:** 3479–3483.
42. Mahley, R. W., T. L. Innerarity, S. C. Rall, and K. H. Weisgraber. 1984. Plasma lipoproteins: apolipoprotein structure and function. *J. Lipid Res.* **25:** 1277–1294.
43. Hui, D. Y., T. L. Innerarity, R. W. Milne, Y. L. Marcel, and R. W. Mahley. 1984. Binding of chylomicron remnants and β-very low density lipoproteins to hepatic and extrahepatic lipoprotein receptors. *J. Biol. Chem.* **259:** 15060–15068.
44. Tam, S. P., and W. C. Breckenridge. 1987. The interaction of lipolysis products of very low density lipoprotein with plasma high density lipoprotein (HDL): perfusate HDL with plasma HDL subfractions. *Biochem. Cell Biol.* **65:** 252–260.
45. Davis, R. A., S. C. Engelhorn, S. H. Pangburn, D. B. Weinstein, and D. Steinberg. 1979. Very low density lipoprotein synthesis and secretion by cultured rat hepatocytes. *J. Biol. Chem.* **254:** 2010–2016.
46. Wilcox, H. G., and M. Heimberg. 1987. Secretion and uptake of nascent hepatic very low density lipoproteins by perfused livers from fed and fasted rats. *J. Lipid Res.* **28:** 351–360.
47. Berry, E. M., R. Aldini, H. Bar-On, and S. Eisenberg. 1981. Role of the liver in the degradation of very low density lipoproteins: a study of lipolysis by heparin releasable liver lipase and uptake during isolated rat liver perfusion. *Eur. J. Clin. Invest.* **11:** 151–159.
48. Windler, H. G., and A. E. Spaeth. 1985. Regulated biosynthesis and divergent metabolism of three forms of hepatic apolipoprotein B in the rat. *J. Lipid Res.* **26:** 70–81.
49. Windler, E., and R. J. Havel. 1985. Inhibitory effects of C apolipoproteins from rats and humans on the uptake of triglyceride-rich lipoproteins and their remnants by the perfused rat liver. *J. Lipid Res.* **26:** 556–565.
50. Bradley, W. A., S-L. C. Hwang, J. B. Karlin, A-H. Y. Lin, S. C. Prasad, A. M. Gotto, and S. H. Gianturco. 1984. Low density lipoprotein receptor binding determinants switch from apolipoprotein E to apolipoprotein B during conversion of hypertriglyceridemic very low density lipoproteins to low density lipoproteins. *J. Biol. Chem.* **259:** 14728–14735.
51. Melish, J., N-A. Le, H. N. Ginsberg, D. Steinberg, and W. V. Brown. 1980. Dissociation of apoprotein B and triglyceride production in very low density lipoprotein. *Am. J. Physiol.* **239:** E354–362.
52. Steiner, G., and M. F. Reardon. 1983. A new model of human VLDL metabolism based on simultaneous studies of apoB and triglyceride. *Metabolism.* **32:** 342–347.
53. Baker, N. 1982. Triglyceride kinetics: experimental problems related to modeling. *In* Lipoprotein Kinetics and Modeling. M. Berman, S. M. Grundy, and B. V. Howard, editors. Academic Press, New York. 253–270.
54. Baker, N. 1984. Plasma triacylglycerol turnover in rats using labeled glycerol. *Lipids.* **19:** 139–141.
55. Trezzi, E., C. Calvi, P. Roma, and A. L. Catapano. 1983. Subfractionation of human very low density lipoproteins by heparin-Sepharose affinity chromatography. *J. Lipid Res.* **24:** 790–795.
56. Evans, A. J., M. W. Huff, and B. M. Wolfe. 1989. Accumulation of an apoE-poor subfraction of very low density lipoprotein in hypertriglyceridemic men. *J. Lipid Res.* **30:** 1691–1701.
57. Winkler, K. E., and J. B. Marsh. 1989. Characterization of nascent high density lipoprotein subfractions from perfusates of rat liver. *J. Lipid Res.* **30:** 979–987.
58. Olefsky, J., J. W. Farquhar, and G. M. Reaven. 1974. Sex differences in the kinetics of triglyceride metabolism in normal and hypertriglyceridemic subjects. *Eur. J. Clin. Invest.* **4:** 121–127.
59. Boberg, J., L. A. Carlson, U. Freyschuss, B. W. Lassers, and M. L. Wahlqvist. 1972. Splanchnic secretion rates of plasma triglycerides and total and splanchnic turnover of plasma free fatty acids in men with normo- and hypertriglyceridemia. *Eur. J. Clin. Invest.* **12:** 454–466.
60. Cortner, J. A., P. M. Coates, N-A. Le, D. R. Cryer, M. C. Ragni, A. Faulkner, and T. Langer. 1987. Kinetics of chylomicron remnant clearance in normal and hyperlipoproteinemic subjects. *J. Lipid Res.* **28:** 195–206.
61. Nestel, P. J., and T. Billington. 1987. Slower catabolism of apoB-48 than apoB-100 in triglyceride-rich lipoproteins during heparin infusions in type 5 hyperlipoproteinemic subjects. *Metabolism.* **36:** 172–175.

Appendix. Table 1. Rate constants for all subjects derived from fitting the model in Fig. 9 to the apoB and triglyceride kinetic data

	Subject			
L(i,j)	F	K	H	J[a]
		h^{-1}		
L(3,1)	0.63	0.75	0.82	1.36
	(0.03)[b]	(0.14)	(0.12)	(0.16)
L(4,1)			0.21	
			(0.001)	
L(5,3)	0.076	0.083	0.087	0.12
	(0.005)	(0.011)	(0.01)	(0.02)
L(6,3)	0.15	0.066	0.110	0.068
	(0.004)	(0.009)	(0.01)	(0.01)
L(7,3)	0.006	0.005	0.007	0.002
	(0.001)	(0.001)	(0.001)	(0.0003)
L(5,4)			0.002	
			(0.001)	
L(6,4)			0.001	
			(0.001)	
L(0,5)	1.24	1.12	0.93	1.18
	(0.041)	(0.092)	(0.086)	(0.015)
L(0,6)	1.24	1.12	0.93	1.18
	(0.041)	(0.092)	(0.086)	(0.015)
L(0,7)	0.82	0.18	0.17	0.26
	(0.07)	(0.06)	(0.02)	(0.04)
L(8,5)		0.098	0.081	0.043
		(0.030)	(0.032)	(0.015)
L(9,6)	0.07	0.098	0.081	0.043
	(0.011)	(0.030)	(0.032)	(0.015)
L(9,5)	0.07			
	(0.011)			
L(10,7)	0.50	0.05	0.14	0.12
	(0.10)	(0.03)	(0.06)	(0.05)
L(0,8)		0.024	0.039	0.057
		(0.018)	(0.019)	(0.017)
L(9,8)	0.21	0.064	0.14	0.032
	(0.005)	(0.019)	(0.022)	(0.010)
L(0,9)	0.20	0.080	0.17	0.080
	(0.005)	(0.002)	(0.003)	
L(10,9)	0.01	0.009	0.02	0.009
	(0.001)	(0.001)	(0.001)	
L(0,10)	0.19	0.07	0.13	0.14
	(0.01)	(0.005)	(0.006)	
L(14,11)		1.22	1.01	1.22
		(0.107)	(0.092)	
L(15,12)	1.31	1.22	1.01	1.22
	(0.041)	(0.107)	(0.092)	
L(15,11)	1.31			
	(0.041)			
L(16,13)	1.32	0.24	0.31	0.39
	(0.09)	(0.08)	(0.09)	(0.16)
L(0,14)			0.039	
			(0.019)	
L(15,14)	0.21	0.089	0.14	0.089
	(0.005)	(0.002)	(0.022)	
L(0,15)	0.11	0.031	0.12	0.025
	(0.005)	(0.002)	(0.003)	
L(16,15)	0.10	0.06	0.06	0.06
	(0.01)	(0.004)	(0.005)	
L(0,16)	0.19	0.07	0.13	0.14
	(0.01)	(0.005)	(0.006)	

L(i,j) for the glycerol section of the model were L(2,1) = 15.6 and L(1,2) = 5.1 h^{-1}; these parameters were not adjustable. The turnover rate (sum of L(i,j)) for compartment 1 was fixed at 34.3 h^{-1}.

[a]ApoB rate constants based upon apoB parameters derived from fitting subject K.

[b]Values in parentheses are ± SD.

Appendix. Table 2. Compartment pool sizes and transport rates derived from the compartmental analysis of each subject's apoB and triglyceride kinetic data

	Subject			
	F	K	H	J[a]
		mg[b]		
M(5)	1860	1550	1510	3140
		(395)	(200)	(380)
M(6)	2340	960	1140	1880
	(170)[c]	(330)	(240)	(240)
M(7)	110	450	270	240
	(9)	(122)	(220)	(105)
M(8)	0.89	1720	675	1530
		(400)	(200)	(380)
M(9)	1385	2305	1040	1460
	(170)	(330)	(240)	(240)
M(10)	360	570	370	310
	(9)	(125)	(210)	(110)
M(11)	43.0	15.9	45.0	16.7
	(0.1)	(1.5)	(3.7)	
M(12)	20.0	11.3	40.0	14.8
	(1.9)	(1.8)	(4.6)	
M(13)	4.40	12.5	30.0	5.70
	(1.3)	(3.5)	(15.0)	(1.8)
M(14)	0.35	220	250	230
	(0.1)	(1.5)	(3.7)	
M(15)	390	375	420	435
	(1.9)	(1.8)	(4.6)	
M(16)	230	335	270	210
	(1.3)	(3.4)	(15.0)	(18.0)
		mg/h[d]		
R(0,5)	2320	1740	1400	3700
	(76)	(410)	(230)	(500)
R(0,6)	2920	1080	1060	2210
	(245)	(350)	(245)	(310)
R(0,7)	93.5	85.0	46.0	64.6
	(14.9)	(27.2)	(27.0)	(21.3)
R(8,5)		153	122	136
		(35)	(35)	(34)
R(9,6)	165	95.0	92.0	82.0
	(16)	(23)	(21)	(21)
R(9,5)	130			
	(20)			
R(10,7)	57.0	21.9	37.6	30.3
	(5.7)	(9.6)	(31.0)	(5.2)
R(9,8)	0.2	110	95.0	48.0
	(0.01)	(15)	(23)	(8.0)
R(10,9)	14.7	19.8	12.2	12.7
	(1.8)	(2.9)	(2.2)	(2.2)
R(0,8)		42.0	27.0	88.0
		(32)	(19)	(36)
R(0,9)	279	178	110	114
	(34)	(28)	(20)	(20)
R(0,10)	71.7	41.7	49.8	43.0
	(5.7)	(10.4)	(30.8)	
R(14,11)		19.4	45.0	21.0
		(0.4)	(0.9)	
R(15,12)	27.0	13.8	40.0	18.0
	(2.0)	(1.7)	(3.8)	
R(16,13)	5.8	2.9	9.3	2.2
	(1.7)	(0.8)	(1.8)	(0.2)
R(15,11)	56			
	(1.8)			
R(15,14)	0.07	20.0	35.0	21.0
	(0.01)	(2.3)	(5.4)	
R(16,15)	39.0	21.8	26.7	27.3
	(2.8)	(1.4)	(2.1)	
R(0,14)			10.0	
			(1.5)	
R(0,15)	44.0	11.5	52.0	11.0
	(3.5)	(1.5)	(2.3)	
R(0.16)	44.9	24.7	36.0	29.5
	(3.0)	(1.7)	(2.9)	(0.25)

[a]ApoB parameters are based upon subject J's pool size with rate constants being based upon those derived from fitting subject K's apoB data.

[b]Total pool size.

[c]Values in parentheses are ± SD.

[d]Not normalized to mg/kg/d.